

# The hydrogen Balmer lines and jump in absorption in accretion disc modeling - an ultraviolet-optical spectral analysis of the dwarf novae UZ Serpentis and CY Lyrae

Patrick Godon,<sup>1,2\*</sup> Edward M. Sion,<sup>1</sup> Paula Szkody,<sup>3</sup> William P. Blair<sup>2</sup>

<sup>1</sup>*Department of Astrophysics and Planetary Science, Villanova University, 800 E. Lancaster Ave., Villanova PA 19085, USA*

<sup>2</sup>*Department of Physics and Astronomy, Johns Hopkins University, 3700 San Martin Dr., Baltimore, MD 21218, USA*

<sup>3</sup>*Department of Astronomy, University of Washington, 3910 15th Ave NE, Seattle, WA 98195, USA*

Accepted XXX. Received YYY; in original form ZZZ

## ABSTRACT

The spectra of disc-dominated cataclysmic variables (CVs) often deviate from the spectra of accretion disc models; in particular, the Balmer jump and absorption lines are found to be shallower in the observations than in the models. We carried out a combined ultraviolet-optical spectral analysis of two dwarf novae: UZ Ser in outburst, decline, and quiescence, and CY Lyr on the rise to outburst and in outburst. We fit the Balmer jump and absorption lines, the continuum flux level and slope by adjusting the accretion rate, inclination, and disc outer radius. For both systems we find an accretion rate  $\dot{M} \approx 8 \times 10^{-9} M_{\odot}/\text{yr}$  in outburst, and  $\dot{M} \approx 2 - 3 \times 10^{-9} M_{\odot}/\text{yr}$  for the rise and decline phases. The outer disc radius we derive is smaller than expected ( $R_{\text{disc}} \approx 0.2a$ , where  $a$  is the binary separation), except during late rise (for CY Lyr) where  $R_{\text{disc}} = 0.3a$ . UZ Ser also reveals a 60,000 K white dwarf. These results show that during a dwarf nova cycle the radius of the disc is the largest just before the peak of the outburst, in qualitative agreement with the disc instability model for dwarf nova outbursts. We suspect that an additional emitting component (e.g. disc wind) is also at work to reduce the slope of the continuum and size of the Balmer jump and absorption lines. We stress that both the outer disc radius and disc wind need to be taken into account for more realistic disc modeling of CVs.

**Key words:** accretion, accretion discs — white dwarfs – stars: dwarf novae — stars: individual: UZ Serpentis, CY Lyrae – novae, cataclysmic variables

## 1 INTRODUCTION

Cataclysmic Variables (CVs) are evolved compact binaries in which a white dwarf (WD) star (the primary) accretes matter from a main (or post-main) sequence star (the secondary) filling its Roche lobe. As a consequence, matter streams from the secondary through the first Lagrangian point into the Roche lobe of the primary. In weakly- and non-magnetic CVs the stream of matter eventually forms an accretion disc around the WD (see Warner 1995, for a review).

Dwarf novae (DNe) are a subclass of non-magnetic CVs found mostly in a state of low accretion, ‘quiescence’, interrupted periodically or sporadically by periods of intense accretion or ‘outbursts’. During an outburst, the mass ac-

cretion rate in DNe reaches  $\dot{M} \sim 10^{-8} - 10^{-9} M_{\odot}\text{yr}^{-1}$ , and the accretion disc peaks in the ultraviolet (UV). During quiescence, the mass accretion rate drops to  $\dot{M} \sim 10^{-11} - 10^{-12} M_{\odot}\text{yr}^{-1}$  and the accretion heated WD, with a temperature  $T_{\text{eff}} \sim 15,000 - 50,000$  K, becomes the dominant source of UV light in the system.

The remaining non-magnetic disc CVs form the nova-like (NL) subclass, and are found predominantly in a state of high accretion. In NLs in high state and DNe in outburst, the accretion disc dominates both the UV and the optical bands. For this reason, disc-dominated DNe in outburst and NLs in high state are ideal laboratories to study accretion discs (e.g. Warner 1995).

However, it was shown (Wade 1984, 1988; Long et al. 1991) that the UV spectral energy distribution (SED) of many disc-dominated CVs systematically disagrees with the standard disc model (Pringle 1981) SED. Standard

\* E-mail: patrick.godon@villanova.edu

disc model SEDs (such as e.g. in Long et al. 1991; Wade & Hubeny 1998; Linnell et al. 2012) were too blue compared to the UV data, with the NLs exhibiting a larger discrepancy than the DNe (la Dous 1991; Linnell et al. 2007, 2008, 2009, 2010; Godon et al. 2017). Alternatively, one can state that the standard disc models that scaled to the correct distance to these CV systems did not provide acceptable chi square ( $\chi^2$ ) fits.

It was suggested (Long et al. 1994; Puebla et al. 2007; Linnell et al. 2010) to revise the disc temperature profile in the innermost part of the disc to help flatten the slope of the UV continuum. Quantitatively, the theoretical SED of the standard disc model was predicted to behave as  $F_\lambda \propto \lambda^{-2.33}$  (Lynden-Bell 1969, who explicitly mentioned *when neglecting the disc edges*). A full disc atmosphere calculation (e.g. Wade & Hubeny 1998), however, gives an UV SED slightly steeper, with  $F_\lambda \propto \lambda^{-2.5} - \lambda^{-3.0}$ . While the difference in results is likely due, in part, to the black body (BB) assumption vs. disc atmosphere calculations, it is also due to the effects of the inner boundary condition creating a maximum in the disc temperature at  $R = 1.36R_0$ , where  $R_0$  is the inner disc radius. In Godon et al. (2017) we showed how the location of the inner radius disc, where the boundary condition is imposed, affects the slope of the FUV continuum (and in the present work, we show how the size of the outer radius of the disc affects the continuum slope in the NUV and optical). Compared to this, DNe have an average UV SED  $F_\lambda \propto \lambda^{-2.25}$ , while NLs are flatter with  $F_\lambda \propto \lambda^{-1.90}$  for UX UMa systems,  $\propto \lambda^{-1.70}$  for VY Scl systems, and  $\propto \lambda^{-1.63}$  for SW Sex systems (see Godon et al. 2017).

At the same time, standard disc model optical spectra exhibit strong Balmer jumps in absorption which are not observed (Wade 1984; la Dous 1989a; Knigge et al. 1998). Instead, a small Balmer jump is seen in absorption in the early phase of the outburst (rise) of DNe, it decreases with time and, as the system reaches quiescence, it is replaced by a Balmer jump in emission together with the low order of the Balmer series also in emission (e.g. Verbunt et al. 1984; Szkody 1985; Thorstensen et al. 1998). As to the disc-dominated NLs, most of the time their spectra show either no Balmer jump at all, or a Balmer jump in emission; and when seen in absorption the amplitude of the jump is rather small (e.g. RW Tri, UX UMa; Williams 1983).

It has been suggested (Matthews et al. 2015, but see also Knigge et al. (1997)) that an accretion disc wind in high-state non-magnetic nova-likes could significantly contribute to the overall UV and optical spectrum. The disc wind adds Balmer continuum emission (a Balmer jump in emission) and flattens the slope of the entire spectrum, thereby improving the spectral fit both in the UV and optical. It has also been proposed (Nixon & Pringle 2019) that large magnetically controlled zones (MCZs, due to the presence of an inverse cascade of magnetic helicity in three-dimensional MHD turbulence; e.g. Shapovalov & Vishniac 2011) could transfer mass and angular momentum outwards, decreasing the temperature in the inner disc ( $R \lesssim 3R_*$ ) while increasing it in the outer disc ( $R \gg R_*$ ), thereby flattening the slope of the spectral continuum in these systems. The time-scale involved in that process is so large that it is predicted to occur in nova-likes remaining in high state for very long periods of time. If that's the case, one would expect UX UMa systems (that never go into a low state) to

have the flattest slope of all, however, their slope (-1.90) is steeper than VY Scl systems (-1.70) and SW Sex systems (-1.63).

In a previous work (Godon et al. 2017), we pointed out an additional factor that has to be taken into account when modeling accretion discs: the increase of the inner radius of the disc (due, e.g., to the presence of a geometrically thick boundary layer) can significantly reduce the inner disc peak temperature, resulting in a UV spectrum with a shallower continuum slope in better agreement with the observations.

In the present work we further model the disc to investigate the effect of the outer radius of the disc spectrum. We show that, at high accretion rate, the size of the disc dictates the amplitude of the Balmer jump in absorption. The outer disc temperature, which is the coldest temperature in the disc, increases with decreasing radius and can be set to reduce the size of the Balmer jump in absorption to fit the optical data of some disc-dominated CV systems. The effect of varying the outer disc size on the spectrum was theoretically investigated in a more general way by Shaviv & Wehrse (1991) and Idan et al. (2010); it was also invoked to explain the poor fit of the standard disc model spectrum to UV and optical spectra of some short period DNe (Hassall et al. 1983). Here, we carry out a UV-Optical spectral analysis of the two DNe UZ Ser and CY Lyr paying particular attention to the size of the outer radius of the disc.

The two DNe UZ Ser and CY Lyr are introduced in the next section; the archival data is presented in section 3; our spectral modeling method is explained in section 4; the results are presented and discussed in section 4, followed by a summary and our conclusions in section 6.

## 2 THE DWARF NOVAE UZ SERPENTIS AND CY LYRAE

**The Z Cam Dwarf Nova UZ Serpentis.** UZ Ser is a Z Cam subtype of DN, namely it exhibits phases when the system remains in an intermediate, “standstill”, state (Dyck 1987, 1989; Honeycutt et al. 1998). From the AAVSO we find that the system can reach a maximum visual magnitude  $m_v = 11.7$  and a minimum as low as  $m_v = 17$ . The system parameters are not well known, but an analysis of the masses and inclination (Echevarría & Michel 2007) favors a mass ratio  $0.3 < q < 0.6$ , a white dwarf mass  $M_{\text{wd}} = 0.9 \pm 0.1M_\odot$ , and a secondary mass  $M_2 = 0.4 \pm 0.1M_\odot$ . As the system does not show eclipses of any kind, it must have a moderate inclination  $i < 65 - 70^\circ$ , and the analysis of Echevarría & Michel (2007, Fig.5 in their manuscript) implies  $i > 38^\circ$  (consistent with the amplitude of the optical modulation (Echevarría 1988)). Therefore, following Echevarría & Michel (2007), we assume here  $i = (50 \pm 10)^\circ$ . With a period of 0.17589 days (a little above 4hr Echevarría & Michel 2007), the binary separation is of the order of  $a \sim 10^{11}$  cm.

The exact distance to the system is not known, as its parallax has not been obtained by Gaia nor by Hipparcos. Assuming a negligible color excess, Herbig (1944) suggested that UZ Ser is located in front of a cloud itself located at a distance of 200-300 pc producing a regional  $E(B - V)$  of 0.4 (Baker & Kiefer 1942). Namely, Herbig (1944) suggested  $d < 200$  pc. That region of the sky, however, is very *patchy* (as can be verified with the Galactic

**Table 1.** Adopted System Parameters

Parameter	UZ Ser	Reference	CY Lyr	References
P (days)	0.17589	Echevarría (1988); Echevarría & Michel (2007)	0.1591	Thorstensen et al. (1998)
$M_{\text{wd}} (M_{\odot})$	$0.9 \pm 0.1$	Echevarría & Michel (2007)	$\sim 0.8$	averaged CV WD mass (Zorotovic et al. 2011)
$M_2 (M_{\odot})$	$0.4 \pm 0.1$	Echevarría & Michel (2007)		
$i$ (deg)	$50 \pm 10$	Echevarría & Michel (2007)	35	this work
$E(B - V)$	0.24	Bruch & Engel (1994); Godon et al. (2017)	0.15	Szkody (1985)
$a (10^5 \text{ km})$	$\sim 10$		$\sim 9$	
$d$ (pc)	$\sim 300\text{-}400$	see text	$490 \pm 10$	Gaia DR2 Prusti et al. (2016); Brown et al. (2018)

dust reddening and extinction map (Schlegel et al. 1998; Schlafly & Finkbeiner 2011)<sup>1</sup>, and for that reason the distance estimate from Herbig (1944) has been deemed unreliable (Echevarría et al. 1981). In addition, the reddening of UZ Ser might not be negligible, it is likely of the order of  $E(B-V)=0.25$  (see next section) and could be as large as 0.30-0.35 (Verbunt 1987).

We use a more recent extinction map for individual objects (Morales-Durán et al. 2015)<sup>2</sup>. In the direct vicinity of UZ Ser (at an angular distance of 8' from UZ Ser) there are three objects with a total extinction  $A(V) \approx 3.5$  (corresponding to  $E(B-V) \approx 1.13$  if we assume  $R = 3.1$ ) located at 2.323 kpc, 2.47 kpc, and  $\sim 3$  kpc. These are consistent with the presence of a second cloud located at a distance of 1-2 kpc adding an extra color excess of +0.5 mag to the first cloud as noted by (Baker & Kiefer 1942). Eight more objects within a one degree radius have a reddening of about 0.4-0.8 with distances between 1.6 and 3 kpc. Within a radius of 2 deg all the objects have  $E(B-V) \geq 0.32$ . There are only a handful of objects at  $d < 1200$  pc (and all with  $d > 300$  pc) and their color excess (as a function of the distance) seems to follow a linear pattern. This could confirm the presence of a first cloud having a color excess of  $\sim 0.3$ , and would imply that UZ Ser, with a color excess of  $\sim 0.25$ , is at the distant edge of (or just behind) the first cloud at a distance  $d \sim 300$  pc. However, due to the paucity of data points for  $d < 1200$  pc and the already mentioned patchiness of the sky in this region, UZ Ser could also be located further away. Urban & Sion (2006) used the correlation between the maximum magnitude of a CV systems and its orbital period to derive a distance of about 280 pc. It is most likely that  $200 \text{ pc} < d < 500 \text{ pc}$ , here we assume:  $d \sim 300 - 400 \text{ pc}$ .

We list all the system parameters we adopted for UZ Ser in Table 1.

In the UV, UZ Ser has only been observed with the *International Ultraviolet Explorer (IUE)* (Echevarría et al. 1981; Verbunt et al. 1984). The continuum slope of the (dereddened) IUE spectra in outburst is rather steep, -3 on a log-log scale [see Godon et al. (2017)]. This makes UZ Ser “bluer” than all CVs in outburst, and indicates the presence of a hot component, possibly the disc at a high  $\dot{M}$ . Even its quiescent IUE spectrum (obtained on Aug 15, 1982) has a rather steep slope, likely due to the heated WD. While most CVs have disc emission with a UV spectral continuum slope too shallow compared to the standard disc model (Puebla et al. 2007; Godon et al. 2017), UZ Ser has a UV

continuum slope comparable to a standard disc model accreting at a high mass accretion rate. Also it exhibits a Balmer Jump of 0.3 mag (Panek 1979) in absorption in the optical, in agreement with the standard disc model and contrary to many disc-dominated CVs. UZ Ser seems to be one of a few systems exhibiting spectral features in good agreement with the standard disc model.

The ephemeris of the system is  $\text{HJD} = 2446622.68149(5) + 0.17589(2)\text{E}$  (phase zero when the backside of the secondary is facing the observer; Echevarría & Michel 2007). However, the error in the period (0.00002) and the number of cycles ( $\sim 10,000$ ) since the IUE observations ( $\text{HJD} \sim 2444463 - 2445197$ ) gives a large orbital phase error  $\sim \pm 0.25 - \pm 0.16$ , making an orbital phase variability analysis impossible. The low S/N of the IUE spectra also prevents an assessment of the absorption line radial velocity.

**The U Gem Dwarf Nova CY Lyrae.** With a period of 0.1591 days (a little less than 4hr; Thorstensen et al. 1998), CY Lyr is classified as a U Gem type dwarf nova. It exhibits relatively short outbursts lasting about 5 days (Szkody & Mattei 1984), during which its magnitude increases from 17.0 to 13.2 (Szkody 1985). Its inclination is unknown, but with a radial velocity  $K_1 = 126 \pm 7 \text{ km/s}$  (Thorstensen et al. 1998) and showing no eclipse of any kind, it is likely that the system is viewed at a moderate inclination. CY Lyr has a Gaia parallax of  $2.04 \pm 0.04 \text{ mas}$  (Prusti et al. 2016; Brown et al. 2018; Eyer et al. 2018; Luri et al. 2018), giving a distance  $d = 490 \pm 10 \text{ pc}$ . The secondary star was estimated to be an M3.5 dwarf assuming a distance of 320 pc (Thorstensen et al. 1998), but the larger Gaia distance implies that the M dwarf is of an earlier type. The mass of the WD is unknown and in the present work we will assume an average CV WD mass of  $\approx 0.8M_{\odot}$  (Zorotovic et al. 2011). Under these assumptions, the binary separation of the system is likely similar to that of UZ Ser, and because of its slightly smaller binary orbital period, we assume here  $a = 9 \times 10^5 \text{ km}$ . All the systems parameters are listed in Table 1.

CY Lyr has a reddening  $E(B-V) = 0.15$ , estimated from the 2175 Å ISM absorption feature in its IUE spectrum (Szkody 1985). The continuum slope of its dereddened IUE spectrum in outburst is -2.5 (on a log-log scale Godon et al. 2017), in good agreement with standard disc model spectra (Wade & Hubeny 1998).

<sup>1</sup> <https://irsa.ipac.caltech.edu/applications/DUST/>

<sup>2</sup> <http://svo2.cab.inta-csic.es/theory/exmap/index.php>

### 3 THE ARCHIVAL DATA

#### 3.1 UZ Serpentis.

UZ Ser has a total of 16 *IUE* spectra (8 SWP & 8 LWR) covering both its outburst and quiescent states. A first (SWP+LWR) spectrum was obtained on 1980 August 12, a day after the system went into a short outburst (Echerrarría et al. 1981). Another single (SWP+LWR) spectrum was obtained on 1981 September 22, within a day of the peak of an outburst. A series of 6 (SWP+LWR) spectra were obtained during the second week of August 1982 as the system was in outburst and declined into quiescence (Verbunt et al. 1984). Details on the archival *IUE* observations are given in Table 2.

The *IUE* Aug 1982 observations were coordinated with simultaneous spectroscopic optical observations (Verbunt et al. 1984) and are therefore of special interest. On 1982 Aug 6 UZ Ser went into outburst (reaching a magnitude of 12.8) and the *IUE* spectra were obtained on Aug 8, 9, 10, 11, 12 & 15, as the system faded back into quiescence. The continuum flux level decreased by a factor of 20 from Aug 8 to Aug 15. We digitally extracted the optical spectra obtained on Aug 11 & 15 from Verbunt et al. (1984), as they coincide (to within about 1/2 hr) with the *IUE* spectra obtained on these dates (see Table 3). Even though Verbunt et al. (1984) did collect more optical data, we were only able to extract those spectra that were displayed in the original publication.

Of all the *IUE* exposures, the 22 Sep 1981 spectrum (SWP15078 & LWR11605) has the highest continuum flux level, about 25 times larger than the 15 Aug 1982 spectrum (SWP17700 & LWR13960) which has the lowest continuum flux level. The AAVSO data indicate that the system possibly reached a visual magnitude of 12.8 on Sep 22, 1981. There is no valid AAVSO data for 15 Aug 1982, but the AAVSO data show a decline from Aug 9 ( $m_v = 13$ ) through Aug 12 ( $m_v = 15$ ), and the *IUE* data show that the UV continuum flux level decreased from  $4.5 \times 10^{-14}$  erg/s/cm<sup>2</sup>/Å on Aug 12 and reached a minimum of  $1.5 \times 10^{-14}$  erg/s/cm<sup>2</sup>/Å on Aug 15 (a drop by a factor of 3). On that day, Aug 12, the visual magnitude was probably close to 17.

Therefore, it is reasonable to assume that the Sep 1981 spectrum is mostly dominated by emission from the accretion disc (mid-outburst), while the Aug 15 spectrum is likely dominated by emission coming mostly from the WD (quiescence).

The mean extinction laws of Savage & Mathis (1979) and Seaton (1979) are commonly used to deredden spectra affected by interstellar extinction, or equivalently the formulation of Cardelli et al. (1989a,b) is used (with a value of  $R_v$  near 3.1-3.2 (Mathis 1990)). In our more recent work we dereddened UV and optical spectra using the extinction law given by Fitzpatrick & Massa (2007).

The interstellar extinction produces a strong and broad absorption feature centred at 2175 Å, due mainly to polycyclic aromatic hydrocarbon (PAH) grains (Li & Draine 2001). PAHs, however, do not dominate the FUV extinction, and the 2175 Å bump correlates poorly with the FUV extinction (Greenberg & Chlewicki 1983): there is a large sample variance about the mean average Galactic extinction curve observed in the shorter wavelength of the FUV. Nevertheless, the reddening is often assessed from the 2175 Å

PAHs feature and gives an accuracy of about 20%. Furthermore, the extinction curve itself is an average throughout the Galaxy and could be different in different directions.

All the above extinction laws have a similar correction from the 2175 Å bump longward of 1,500 Å, but at shorter wavelength Cardelli's gives a higher correction, Seaton and Savage & Mathis gives a smaller correction, and Fitzpatrick & Massa's gives an intermediate correction (as already noted by Selvelli & Gilmozzi 2013). This discrepancy increases with decreasing wavelength. It has been shown (Sasseen et al. 2002) that in the FUV the observed extinction curve is actually consistent with an extrapolation of the standard extinction curve of Savage & Mathis (1979). Consequently, in the present work, we slightly modify our dereddening software (based on Fitzpatrick & Massa (2007) analytical expression) to agree with an extrapolation of Savage & Mathis (1979) in the FUV range.

Based on the 2175 Å absorption feature, the reddening toward UZ Ser has been estimated to be as low as 0.1 (Echerrarría et al. 1981) and as large as 0.35 (la Dous 1991). We derive a reddening value  $E(B-V)=0.24$  for the Sep 1981 *IUE* spectrum (with the highest continuum flux level), and  $E(B-V)=0.30$  for the Aug 08, 1982 spectrum (when the system was in outburst). The region of the LWR *IUE* spectra in the vicinity of the 2175 Å absorption feature is rather noisy with what looks like deep absorption lines. While some of these absorption features might be actual absorption lines (e.g. Si I 1983-6, He II 2053 & 2306, C III 2297), other features might be artifacts. Binning the spectra to 15 Å to derive the reddening (a usual practice; Verbunt 1987) might therefore over estimate the reddening by increasing the 2175 Å feature with these absorption lines and artifacts. We here adopt the  $E(B-V)=0.24$  value as it was obtained from the most reliable spectrum (highest continuum flux level) and it is also consistent with the (average) value given in Bruch & Engel (1994). We note that Verbunt et al. (1984) also found  $E(B-V)=0.30$  for the Aug 08, 1982 spectrum. The LWR spectra obtained in late decline and quiescence are far too noisy to derive  $E(B-V)$  from the 2175 Å absorption feature. We deredden the spectra assuming  $E(B-V)=0.24$ .

We present the SWP15078 & SWP17700 spectra in Fig.1 identifying some absorption and emission lines. The outburst spectrum displays absorption lines from Si III (1192 Å), N V (1240 Å), C II (1335 Å), Si IV (~1400 Å), C IV (~1550 Å), and C III (1621 Å); the absorption feature around 1303 Å is a combination of Si III and O I lines. The depression in the continuum flux near 1720 Å is due to N IV (1719 Å), but also likely to be Si IV (1723 Å), C II (1721 Å), and Si II (1711 Å). There is also a possible absorption line of O V (1371 Å) as well as a forbidden emission line of C III] (1909 Å).

The quiescent spectrum has a lower S/N and the identification of lines is less reliable. It shows many lines in emission and fewer lines in absorption. We identify the Si III + O I (~ 1300 Å) and C II (1335 Å) absorption features, as well as the following emission lines: Ly  $\alpha$  (most probably geo-coronal in origin), N V (1240 Å), Si IV (1400 Å), C IV (1550 Å), He II (1640 Å), Al III (1855 Å), and the forbidden C III] (1909 Å). The spectrum presents several regions with broad absorption features, which could be due to C III (near 1620 Å) and N IV (near 1720 Å). However, these absorption features are very broad, and are more likely due to an ab-

**Table 2.** Archival *IUE* Observation Log

System Name	Short Wave	Long Wave	Date (UT) mmm-dd-yyyy	Time (UT) hh:mm:ss	Exp. Time seconds	SWP Flux (relative)	Fig. #
UZ Ser	SWP09769	LWR08489	Aug 12 1980	00:31:42	2400/1200	15	
	SWP15078	LWR11605	Sep 22 1981	18:41:43	2400/2100	23	9,10
	SWP17633	LWR13901	Aug 08 1982	19:02:28	2400/3600	20	1,11
	SWP17645	LWR13909	Aug 09 1982	23:43:46	3600/3300	17	
	SWP17652	LWR13917	Aug 10 1982	19:13:49	4200/4200	14	
	SWP17661	LWR13922	Aug 11 1982	18:52:20	4800/3600	7.4	1,11
	SWP17672	LWR13930	Aug 12 1982	20:22:17	7800/4800	3.3	
	SWP17700	LWR13960	Aug 15 1982	18:20:10	10800/5400	1.0	1,11
CY Lyr	SWP21030	LWR16779	Sep 12 1983	22:09:45	3600/2400	—	3,4,12
	SWP21058	LWR16794	Sep 15 1983	03:10:16	2520/1800	—	3

**Table 3.** Optical Data Timing

System Name	Date (UT) mmm-dd-yyyy	RJD <sup>a</sup> <i>IUE</i> SWP	RJD <sup>a</sup> <i>IUE</i> LWR	RJD <sup>a</sup> Optical	Optical Flux <sup>b</sup> (relative)	Fig. #
UZ Ser	Aug 08 1982	45190.32	45190.37	—	—	
	Aug 09 1982	45191.53	45191.47	—	—	
	Aug 10 1982	45192.40	45192.35	—	—	
	Aug 11 1982	45193.39	45193.33	45193.36	5.0	11
	Aug 12 1982	45194.44	45194.50	—	—	
	Aug 13 1982	—	—	45195.41	2.0	
	Aug 15 1982	45197.39	45197.46	45197.37	1.0	11
CY Lyr	Oct 09 1982	—	—	45252.00	1.05	4,12
	Jun 25 1997	—	—	50625.00	—	
	Jun 29 1997	—	—	50629.00	—	
	Jun 30 1997	—	—	50629.67	—	
	Jun 30 1997	—	—	50629.74	—	
	Jun 30 1997	—	—	50629.79	—	
	Jun 30 1997	—	—	50629.85	—	
	Jun 30 1997	—	—	50629.90	0.41	4
	Jun 30 1997	—	—	50629.97	0.66	4,13
	Jul 01 1997	—	—	50630.85	1.0	4,12

 (a) RJD=relative Julian Date starting at JD=2,400,000. (b) The relative optical flux is measured in the vicinity  $\lambda \in [4000, 5000]\text{\AA}$  and it is different for each system.

sorbing “iron curtain” (Horne et al. 1994). We identify three such regions where there is a multitude of Fe II lines: near  $\sim 1560\text{-}1590\text{\AA}$ ,  $\sim 1612\text{-}1635\text{\AA}$ , and  $\sim 1709\text{-}1725\text{\AA}$ . The iron curtain is known to dominate the region between  $\sim 1500\text{\AA}$  and  $\sim 1700\text{\AA}$  (e.g. Smith et al. 1994; Pala et al. 2017). The last two regions could also have absorption lines from C III, Si IV and N IV as in the outburst spectrum.

Veiling curtains are fairly common in spectra of CVs and could be due e.g. to stream disc overflow material (Godon 2019) and/or to an outflow (disc wind; Knigge et al. 1997). The fact that we derive a reddening of 0.24 for the Sep 1981 spectrum and 0.30 for the Aug 08, 1982 spectrum is a possible indication that the source is subject to intrinsic reddening. This would also be consistent with veiling. As a consequence, in the Results Section we also discuss how a possible uncertainty of about  $\pm 0.05$  in the reddening, say  $E(B - V) = 0.2$  vs.  $E(B - V) = 0.3$ , translates into an uncertainty in the parameters derived from our spectral analysis.

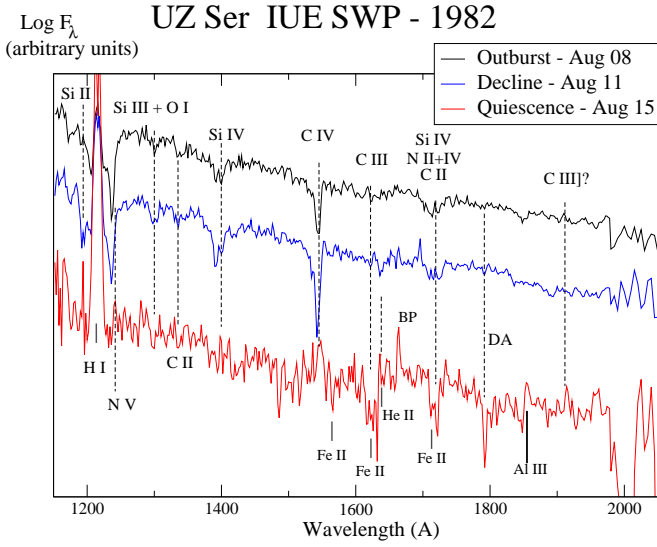


**Figure 1.** The dereddened *IUE* SWP Spectra of UZ Ser in outburst (SWP17633/Aug 08, in black), decline (SWP17661/Aug 11, in blue) and quiescent (SWP17700/Aug 15, in red) are shown (for clarity) on an arbitrary logarithmic scale ( $\text{Log}(F_\lambda)$ , where  $F_\lambda$  is in  $\text{erg/s/cm}^2/\text{\AA}$ ). The most common absorption lines have been marked. There is also a possible forbidden C III emission line around  $\sim 1910 \text{ \AA}$ . The quiescent spectrum exhibits some absorption features that appear to be consistent with absorption from an iron curtain (marked with Fe II below the spectrum). There is a detector artifact (“DA”) just before  $1800 \text{ \AA}$ , and a bad pixel (“BP”) near  $1660 \text{ \AA}$ .

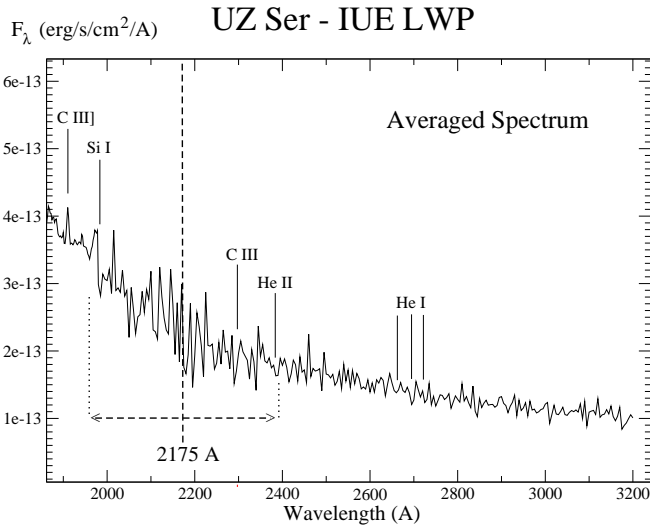


**Figure 2.** The dereddened *IUE* LWR co-added spectrum of UZ Ser. The 8 LWR spectra have been co-added to increase the S/N. We tentatively identify some absorption lines as marked. The spectra were dereddened using the ISM polycyclic aromatic hydrocarbon (PAH)  $2175 \text{ \AA}$  absorption feature. The location of the  $2175 \text{ \AA}$  feature is marked with a vertical dashed line. Note that the spectrum is very noisy within  $\pm 200 \text{ \AA}$  in this region (marked with arrows), making the dereddening more difficult.

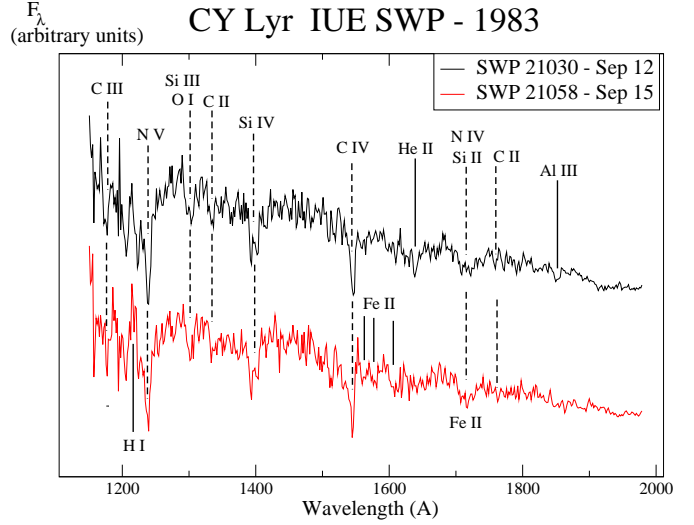


**Figure 3.** The dereddened *IUE* SWP spectra ( $F_\lambda$  vs.  $\lambda$ ) of CY Lyr in outburst displayed on an arbitrary scale. The Sep 15 spectrum is in red and the Sep 12 spectrum is in black. Though the two spectra have about the same flux level, for clarity, they have been displayed on an arbitrary scale so as to not overlap. The most common absorption lines have been identified as marked. The Sep 15 spectrum has a continuum flux level about 10-15% lower than the Sep 12 spectrum and displays some additional absorption lines reminiscent of the iron curtain (see Fig.1 for comparison).

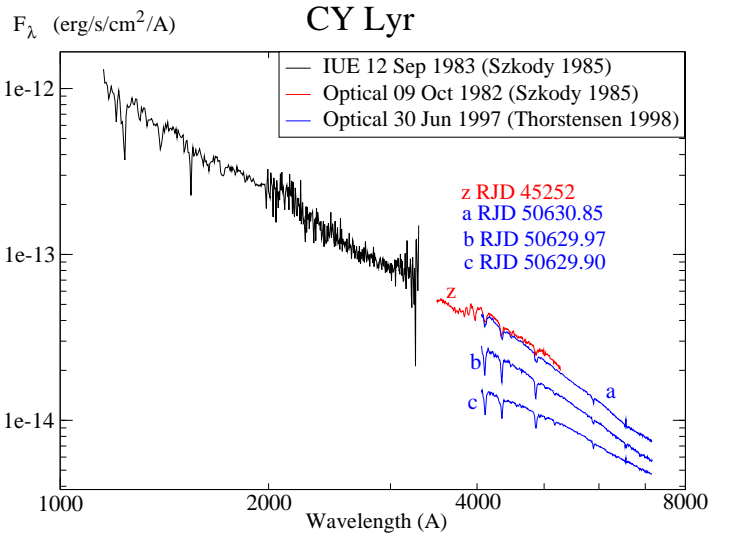


**Figure 4.** The optical spectra of CY Lyr compared to the *IUE* spectrum. All the spectra have been dereddened. The *IUE* spectrum was obtained near outburst maximum light, the 1982 optical spectrum (z) was obtained during outburst, and the 1997 optical spectra were obtained on the rise to outburst (b & c) and in outburst (a).

### 3.2 CY Lyrae.

CY Lyr was observed in the FUV with *IUE* 4 days into outburst (Sep.12-15, 1983, see Table 2), as well as in the optical ( $\sim 3,500 - 5,300 \text{ \AA}$ ) both in quiescence (Oct. 6, 1982) and in outburst (Oct. 9, 1982 [Szkody 1985](#), see Table 3). The optical spectra during the rise to outburst and decline show narrow emission-line cores within the broad Balmer absorption. On Sep. 15 the *IUE* spectrum reveals a P Cygni feature in C IV ( $1500 \text{ \AA}$ ) with the absorption component stronger than the emission component (with no emission component from other lines) which is not seen on Sep 12 at the beginning of the outburst (see Fig.3). The *IUE* LWR spectra of CY Lyr are *unremarkable and rather noisy*, but provide a continuum flux level that can be used in the spectral modeling. The outburst *IUE* and optical spectra are presented together in Fig.4.

CY Lyr was also observed in the optical by [Echevarría & Costero \(1983\)](#), on 7 & 8 Aug 1981) who presented a spectrum that just covers the Balmer Jump from  $\sim 3,800 \text{ \AA}$  to  $\sim 5,500 \text{ \AA}$  with a continuum flux level about twice as large as in [Szkody \(1985\)](#), but with a lower resolution. The absorption lines depth and Balmer Jump amplitude (also in absorption) are similar in both observations, however, the optical spectrum in [Szkody \(1985\)](#) covers the continuum down to  $\sim 3,500 \text{ \AA}$ , which allows a better assessment of the amplitude of the Balmer Jump as it includes the continuum between  $3,500 \text{ \AA}$  and  $3,800 \text{ \AA}$  that can be modeled.

CY Lyr was further observed at the end of June 1997 by [Thorstensen et al. \(1998\)](#), see Table 3), who obtained 8 optical spectra ( $\sim 4,000 - 7,300 \text{ \AA}$ ) almost every hour while the system evolved from quiescence into outburst. The quiescent state spectrum of CY Lyr is typical of quiescent dwarf novae with sharp emission lines, and the secondary is believed to contribute a significant fraction of the continuum flux level ( $\sim 1/6$  at  $6,500 \text{ \AA}$ ). Besides a component from the secondary, the quiescent optical spectrum also contains emission lines and possibly some additional continuum contribution. As the system rises into outburst, the continuum flux level increases, the spectrum becomes bluer, and the emission lines are replaced by absorption lines. The absorption lines are strongest before maximum light, though  $H\alpha$  does display very weak emission. In Fig.4 we display the last 3 optical spectra as the system reached its outburst level. Spectrum (a) is one day into outburst and matches remarkably well the optical spectrum (z) [also shown here in Fig.4] from [Szkody \(1985\)](#). Spectrum (b) was obtained  $\sim 21\text{hr}$  before (a), and spectrum (c) was obtained  $\sim 1\text{hr}40\text{m}$  before (b). Spectrum (b) displays the deepest absorption lines and is likely to have no or minimum emission lines.

These observations reveal that during quiescence the Balmer lines and jump are seen in emission, and the spectral slope of the continuum is rather flat. As the system rises into outburst, the spectral slope becomes steeper (the spectrum becomes bluer), and absorption lines start to dominate the spectrum. The absorption lines are strongest before the system reaches its maximum, then as the system remains in outburst, narrow emission line cores appear within the broad Balmer absorption and the C IV line starts to display a P Cygni profile. These are signs of an outflow (a possible disc wind), and, together with the absorption features from

a possible “iron curtain” (Fig.3), we suspect that here too (as for UZ Ser) there is material over the disc in the line of sight of the observer originating from either a disc wind and/or stream disc overflow, or both.

## 4 SPECTRAL MODELING

### 4.1 TLUSTY

We use the FORTRAN suite of codes TLUSTY, SYNSPEC, ROTIN and DISKSYN (often simply referred to as TLUSTY Hubeny 1988; Hubeny et al. 1994; Hubeny & Lanz 1995) to generate synthetic spectra of stellar atmospheres and discs. The codes include the treatment of hydrogen quasi-molecular satellite lines (low temperature), and LTE/NLTE options. TLUSTY generates a stellar atmosphere model for a given effective surface temperature  $T_{\text{eff}}$  (in K), gravity  $\text{Log}(g)$  (Log of cgs), and chemical composition (in solar units). Using the output from TLUSTY, SYNSPEC generates a continuum with absorption lines. In the present case we do not generate emission lines. For disc spectra we use solar abundances and for stellar spectra we vary abundances as needed. An introductory guide, a reference manual and an operational manual to TLUSTY and SYNSPEC have been released and are available for full details of the codes (Hubeny & Lanz 2017a,b,c).

### 4.2 Synthetic WD stellar atmosphere spectra

The code TLUSTY is first run to generate a one-dimensional (vertical) stellar atmosphere structure for a given surface gravity ( $\text{Log}(g)$ ), effective surface temperature ( $T_{\text{eff}}$ ) and surface composition of the star. Computing a single model is an iterative process that is brought to convergence. In the present case, we treat hydrogen and helium explicitly, and treat nitrogen, carbon and oxygen implicitly (Hubeny & Lanz 1995).

The code SYNSPEC is then run, using the output stellar atmosphere model from TLUSTY as an input, and generates a synthetic stellar spectrum over a given (input) wavelength range. Here we use its full capability and set the spectral range to cover the FUV and optical: from 900 Å to 7500 Å. The code SYNSPEC derives the detailed radiation and flux distribution of continuum and lines and generates the output spectrum (Hubeny & Lanz 1995). SYNSPEC has its own chemical abundances input to generate lines for the chosen species. For temperatures above 35,000 K, we turn on the approximate NLTE treatment of lines in SYNSPEC.

Rotational and instrumental broadening as well as limb darkening are then reproduced using the routine ROTIN. Synspec also generate the specific intensities for a given angle of inclination, which can then be translated into flux. In this manner we have already generated a grid of WD synthetic spectra covering a wide range of temperatures and gravities with solar composition.

For temperature below  $\sim 10,000$  K (and low gravity,  $\text{Log}(g) \sim 4$ ), we turn on the Grey stellar atmosphere option in TLUSTY/SYNSPEC. For temperatures below 6000 K, we use Kurucz solar abundances stellar atmosphere models (e.g. Kurucz 1979). We also use these low temperature solar-abundances stellar spectra to model the secondary and/or the outer accretion disc when the temperature and the effective surface gravity are much lower than that of the WD.

In Fig.5 we present some synthetic stellar atmosphere spectra for a temperature ranging from 3,500 K (with  $\text{Log}(g) = 4$ ) to 45,000 K (with  $\text{Log}(g) = 8$ ). The hydrogen Balmer absorption lines (series) form as the hydrogen atom

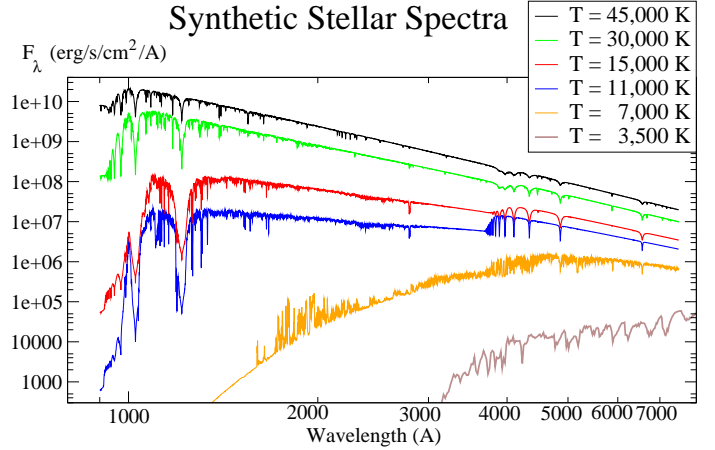


**Figure 5.** Stellar spectra ( $F_{\lambda}$  vs  $\lambda$  on a log-log scale) from 3,500 K to 45,000 K, for temperatures as shown in the upper right panel. The Balmer Jump in absorption, around  $\sim 3,500$ -4,000 Å, is more prominent for temperatures in the range 10-15,000 K. We generate synthetic stellar spectra using TLUSTY/SYNSPEC from 900 Å to 7500 Å for a temperature ranging from  $\sim 10,000$  K to  $\sim 100,000$  K, below  $\sim 10,000$  K we use the Grey atmosphere option in TLUSTY/SYNSPEC, below 6000 K we use Kurucz models.

electron transitions from levels  $n \geq 3$  down to level  $n = 2$ . As  $n$  approaches infinity, it creates a continuous absorption feature appearing as a jump (step) in the continuum flux level in the vicinity  $\lambda \approx 3750$  Å (Fig.5). The Balmer jump in absorption is especially prominent in stellar spectra when the temperature is in the range 8 – 15,000 K. This is important, as the disc can be modeled as a collection of rings, each with a given temperature, and the resulting amplitude of the Balmer jump in the disc itself depends on the lowest temperature in the disc (see next subsection).

### 4.3 Synthetic disc model spectra

Our disc model is based on the Shakura-Sunyaev alpha disc model (the *standard disc model*, Shakura & Sunyaev 1973; Lynden-Bell & Pringle 1974). The disc is assumed to be optically thick, geometrically thin (in the vertical dimension), rotating at a nearly Keplerian speed ( $\Omega \approx \Omega_K$ ), and axisymmetric. The energy dissipated by the Keplerian shear (between adjacent rings of matter) is radiated locally, and the resulting effective surface temperature is consequently solely a function of the radius  $R$ :  $T(R)$  (one-dimensional, e.g. Pringle 1981).

Since the disc has to adjust to the slowly rotating white dwarf, its angular velocity has to decrease and, therefore, a no-shear condition ( $d\Omega/dR = 0$ ) is set at the disc's inner boundary  $R_0$ . As a consequence, the temperature profile reaches a maximum at  $r \approx 1.36R_0$  and decreases to zero as  $R \rightarrow R_0$ . In the standard disc model:  $R_0 = R_{\text{wd}}$ . The validity of such an inner boundary condition might be questioned, especially since it dictates the angular momentum transfer (AMT) from the disc to the star. A decrease in AMT, e.g. setting  $R_0 \rightarrow 0$  (la Dous 1989b) or  $d\Omega/dR < 0$  (Mummery & Balbus 2019), increases the luminosity and

temperature in the inner disc. In CVs the largest effect of such a boundary condition is in the unobservable EUV wavelengths (la Dous 1989b). On the other hand an increase in AMT (if one sets  $R_0 > R_{\text{wd}}$ , Godon et al. 2017) will decrease the luminosity and temperature in the inner disc. The resulting slope of the disc spectral continuum is shallower for an increased AMT and steeper for a decreased AMT. Here we simply assume the no-shear boundary condition at the inner radius of the disc which is set at  $R_0 = R_{\text{wd}}$ .

The standard disc model further assumes that the boundary layer between the star and disc (where the remaining accretion energy is released) is very thin and radiates mainly in the X-ray and EUV. In some previous work (e.g. Godon et al. 2012) we modeled the boundary layer as a hot inner ring in the disc, or alternatively as a hot equatorial belt on the WD surface. This modeling is needed and possible when analyzing *Far Ultraviolet Spectroscopic Explorer (FUSE)* spectra of CVs (going down to 900 Å). However, the modeling diverges for *IUE* spectra, since the higher orders of the Lyman series (i.e. Ly $\beta$ , Ly $\gamma$ , ...) are needed to differentiate between a hot WD, a fast rotating belt, and/or a hot ring/inner disc. In the present work, an increase of the WD temperature is enough to help fit a steep spectral slope (see Results Section).

In our modeling, the white dwarf mass ( $M_{\text{wd}}$ ), the mass accretion rate ( $\dot{M}$ ), the binary inclination ( $i$ ), the inner disc radius ( $R_0$ ), and the outer disc radius ( $R_{\text{disc}}$ ) are all input parameters. Due to the tidal interaction of the secondary star, the maximum size of the accretion disc is expected to be between  $0.3a$  (where  $a$  is the binary separation) for a mass ratio  $q = M_2/M_1 \approx 1$ , and about  $0.6a$  for  $q \ll 0.1$  (Paczynski 1977; Goodman 1993), though in the present work,  $R_{\text{disc}}$  is found by fitting the data.

In Fig. 6 we display the temperature profile  $T(R)$  for two accretion discs around a  $0.8M_{\odot}$  WD with a radius  $R_{\text{wd}} = 7,000$  km: one with  $\dot{M} = 10^{-8}M_{\odot}/\text{yr}$ , and one with  $\dot{M} = 10^{-8.5}M_{\odot}/\text{yr}$ . In these models the inner boundary of the disc is set at  $R_0 = R_{\text{wd}}$  and the outer boundary can be set at different radii (e.g. points 1, 2, 3, etc.). Setting the outer radius of the disc determines the lowest temperature in the disc (note that because our disc rings have a finite thickness, the disc temperature at  $R_0$  takes the temperature of the inner ring:  $T(R_0) = T(R_1) > 0$  K; see below and see Fig. 6).

We divide the disc model into  $N$  rings of radius  $R_i$  ( $i = 1, 2, \dots, N$ ). Each ring has a temperature ( $T(R_i)$ ), density and effective vertical gravity obtained from the disc model for a given stellar mass ( $M_{\text{wd}}$ ), inner and outer disc radii ( $R_0$  &  $R_{\text{disc}}$ ), and mass accretion rate ( $\dot{M}$ ).

We generate a one-dimensional vertical structure for each ring using TLUSTY. For the disc ring the input is the local mass accretion rate, mass of the accreting star, the inner radius of the disc, and radius of the ring in units of the inner radius of the disc.

SYNSPEC is then used to create a spectrum for each ring, and the resulting ring spectra are integrated into a disc spectrum using the code DISKSYN, which includes the effects of (Keplerian) rotational broadening, inclination, and limb darkening. The general procedure we follow to generate disc spectra using TLUSTY can be found in Wade & Hubeny (1998), and our current disc spectra modeling in the UV is given in Godon et al. (2017).

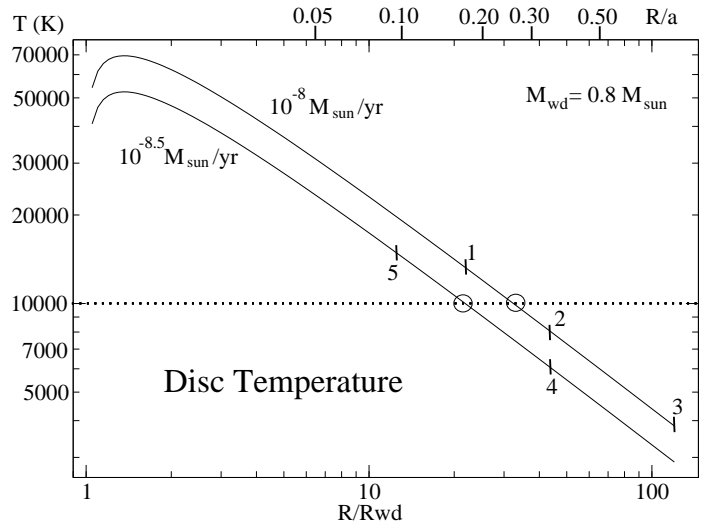


**Figure 6.** The effective surface temperature of the accretion disc model is shown as a function of the radius on a log-log scale. Two mass accretion rates are displayed:  $\dot{M} = 10^{-8}M_{\odot}/\text{yr}$  (upper graph), and  $\dot{M} = 10^{-8.5}M_{\odot}/\text{yr}$  (lower graph). The central WD has a mass  $M_{\text{wd}} = 0.8M_{\odot}$  and a radius  $R_{\text{wd}} = 7,000$  km. The location of the outer disc radius (e.g. 1, 2, 3, etc..) sets the lowest temperature in the disc. The horizontal dotted line shows the outer radii for  $T=10,000$  K where it intersects the graphs. This is the temperature for which the Balmer jump is the strongest. All the Wade & Hubeny disc models (with spectral range 900 Å–2000 Å) are cut off at this radius since the outer colder disc is not expected to contribute much at  $\lambda < 2000$  Å. A disc with an outer radius at (e.g.) (1) or (5) will have a much smaller Balmer jump than a disc with an outer radius at (e.g.) (2), (3), or (4). Above the panel we indicate the size of the accretion disc as a fraction of the binary separation ( $a$ ) in UZ Ser.

We recently extended our modeling to include the optical range (e.g. Darnley et al. 2017; Godon et al. 2018). Accretion disc models in the FUV (say 900–2000 Å) are usually limited to an outer radius where the temperature reaches  $\sim 10,000$  K (shown in Fig. 6 with a dotted line), as lower temperatures contribute very little flux in that spectral range (Wade & Hubeny 1998). However, as one considers the optical range up to 7500 Å, the accretion disc has to be extended to a larger radius to include the colder outer disc (see Fig. 6) contributing to the optical. Here, we incorporate the option to include disc rings as cold as 3,500 K when needed. For disc ring temperatures below  $\sim 6,000$  K (and above  $\sim 3,500$  K), we use Kurucz stellar spectra of appropriate temperature and surface gravity as mentioned in the previous sub-section.

The important spectral features when modeling the disc in the optical are (i) the amplitude of the Balmer jump, (ii) the depth of the hydrogen Balmer lines, and (iii) the slope of the continuum.

We first check the effect of the size of the disc (i.e.  $R_{\text{disc}}$ ) for an  $0.8M_{\odot}$  WD (nearly the average CV WD mass Zorotovic et al. 2011) accreting at a rate  $\dot{M} = 10^{-8}M_{\odot}/\text{yr}$  (for a DN in outburst). The temperature profile for this disc model is shown in Fig. 6 (upper graph). We consider two outer disc radii:  $R_{\text{disc}} = 147,000$  km (# 1 in Fig. 6) with a temperature  $T = 13,342$  K; and  $R_{\text{disc}} = 840,000$  km (# 3 in Fig. 6) with a temperature  $T = 3837$  K. We find (see

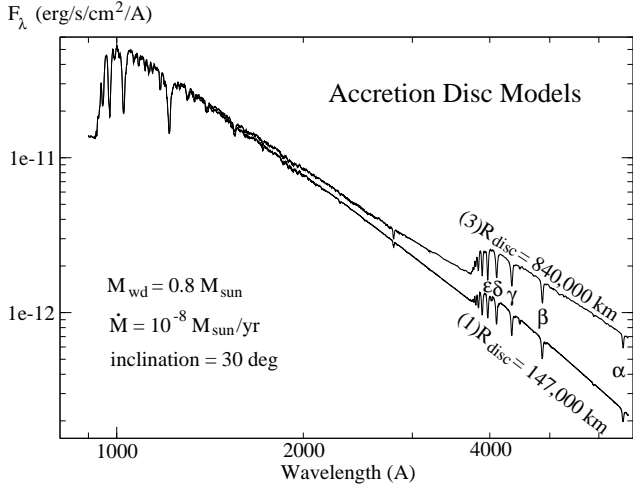


**Figure 7.** Two accretion disc spectra ( $F_\lambda$  vs  $\lambda$  on a log-log scale) generated using TLUSTY/SYNSPEC are displayed. The two discs are identical (with a central  $0.8M_\odot$  white dwarf, a mass accretion rate  $\dot{M} = 10^{-8}M_\odot/\text{yr}$ , and viewed at an inclination  $i = 30^\circ$  for a distance of 100 pc). The outer radius in the first disc has been set to 840,000 km, and the outer ring reaches a temperature of 3837 K (corresponding to model # 3 in Fig.6). In the second disc the outer radius has been set to 147,000 km, and the outer ring reaches a temperature of 13,342 K (corresponding to model # 1 in Fig.6). The amplitude of the Balmer jump as well as the slope of the continuum in the longer wavelengths both depend on the temperature and, therefore, size of the outer disc.

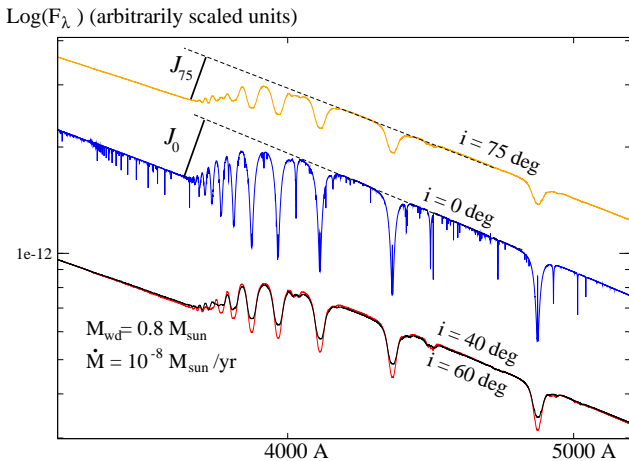


**Figure 8.** The Balmer region is shown for four inclination angles:  $0^\circ$  (in blue in the middle),  $40^\circ$  (in red) superposed to  $60^\circ$  (in black, bottom), and  $75^\circ$  (in orange at the top). For convenience the spectra have been shifted on a log-log scale. From  $i = 0^\circ$  to  $i = 75^\circ$  the Balmer jump decreases by  $\sim 25\%$  ( $J_{75} \approx 0.75J_0$ ), while the absorption lines decrease by  $\sim 80\%$ . For an inclination  $i$  varying from  $\sim 40^\circ$  to  $\sim 60^\circ$  (as considered in the present work), the *relative* depth of the Balmer absorption lines depends strongly on the inclination, however, the amplitude of the Balmer jump and the slope of the continuum are barely affected.

Fig.7) that the amplitude of the Balmer jump decreases significantly as the radius of the disc is decreased from 840,000 km to 147,000 km, corresponding to an increase of almost 10,000 K of the outer disc temperature. This is due to the fact that model (1) has a temperature well above 10,000 K everywhere in the disc (Fig.6). In addition, the slope of the continuum in the optical (and somewhat in the near UV) becomes steeper as the outer radius of the disc decreases, as already noted by [Hassall et al. \(1983\)](#), but little change occurs in the FUV. However, the depth of the Balmer absorption lines remains nearly the same. We note that for a secondary mass  $M_2 = 0.3M_\odot$ , and assuming an outer disc radius of about  $a/3$  (33% the binary separation), the discs shown in Fig.7 would belong to a binary with an orbital period of 19 hr (larger disc) and 1.5 hr (smaller disc).

Next, we check how the inclination affects the disc spectra. We find (see Fig.8) that the Balmer jump is not affected by the inclination as much as the depth of the hydrogen Balmer lines, which strongly decrease with increasing inclination. In the disc modeling there are three main factors affecting the spectrum as the inclination (i) increases: (a) the geometric foreshortening of the flat disc (reducing the continuum flux level by a factor  $\mu = \cos(i)$ ); (b) the dependence of specific intensity ( $I_\nu(\mu)$ ) on the inclination (due to scattering); and (c) the Keplerian velocity broadening (see [la Dous 1989b](#); [Wade & Hubeny 1998](#); [Hubeny & Lanz 2017b](#)). The depth of the absorption lines are affected mainly by (c) and also to some extent by (b); while the *relative* size of the Balmer jump is affected only by (b), which is stronger at higher inclinations.

Consequently, as the mass accretion rate is found mainly by fitting the FUV for a given white dwarf mass and inclination, the inclination (if unknown) and the size of the disc can be found when extending the fit into the optical.

#### 4.4 Fitting Technique.

In our past research we have used three methods to find the model that best fits the data.

(i) The chi square ( $\chi^2$ ) method, which is meaningful when a  $\chi^2$  value is found to be significantly smaller (in a statistical sense) for one model compared to the other models. Because this method is quantitative it is often the *preferred* one.

(ii) The best-fit model can also be found by visual inspection of the fit (see e.g. [Linnell et al. 2007, 2008, 2009, 2010](#)). This qualitative method is used with common sense and can be as effective as (i): it can lead to the same results within the errors and/or uncertainties. Namely, the models that visually appear to deviate from the observed spectrum give significantly higher  $\chi^2$  values

(iii) Fitting all the parameters simultaneously. When the systems parameters (inclination, distance, reddening, WD mass and radius, ..) are known (with a given accuracy), then the best fit is simply the model which scales to the known distance (for e.g. for a given WD temperature for a DN in quiescence, or for a given mass accretion rate for a disc dominated system).

More often than one would like, there can be a discrepancy between the best fit obtained from (i) or (ii) and that derived from (iii). For example, the FUV analysis of VW Hyi after a superoutburst ([Long et al. 2009](#)) revealed that

the scaled radius of the WD is smaller than expected (and even more so with new Gaia distance of 54 pc). And more importantly, the fact that (distance-scaled) disc model fits to disc-dominated CVs are too blue compared to UV spectra (see Introduction) is itself a sign that the scaled model fits do not provide the least chi square fits, or alternatively: the least chi square model fits give the wrong distance. It is important to also note that for UZ Ser, method (i) yielded an inclination  $i = 18^\circ$  in Hamilton et al. (2007) and  $i = 75^\circ$  in Lake & Sion (2001).

For best results, either technique (i) or (ii) has to be combined with technique (iii).

In the present work we pay particular attention to the continua: we choose the model fit exhibiting a continuum that overlaps the observed the continuum (i.e. we do not inspect the absorption lines fit unless we explicitly mention that as in sec.5.2.2.), especially in those portions of the spectrum that have a higher S/N (such as the IUE SWP when compared to the IUE LWR). We also ignore the emission lines and the contaminated Lyman  $\alpha$  region. Consequently, in the present work we choose to use method (ii) and (iii) to derive the goodness of fit, namely we use a *qualitative* method rather than a *quantitative* one.

Using method (iii), the uncertainties of the system parameters translate into uncertainties in the derived mass accretion rates and WD temperature. These uncertainties, which we add using the  $\pm$  sign, reflect the approximate range over which good fits are found over the range of values of the parameters (these uncertainties are not Gaussian distributed errors).

## 5 RESULTS AND DISCUSSION

### 5.1 UZ Ser

#### 5.1.1 The Sep 1981 peak outburst: the SWP15078 spectrum.

We start by considering the highest flux IUE spectrum of UZ Ser obtained on Sep 22, 1981. Hamilton et al. (2007) first modeled the SWP15078 segment with a disc from the grid of disc models of Wade & Hubeny (1998). The Wade & Hubeny (WH for short) disc models are computed for a WD mass taking values of 0.35, 0.55, 0.80, 1.03, and  $1.21M_\odot$ , and the inclination is fixed to  $i=18^\circ, 41^\circ, 60^\circ, 75^\circ$ , and  $81^\circ$ . Using the  $1.03M_\odot$  WD mass disc models (with a radius of 5180 km), Hamilton et al. (2007) obtained a mass accretion rate  $\dot{M} = 2 \times 10^{-8}M_\odot/\text{yr}$  scaling to a distance of 300 pc. In their modeling, they didn't include the possible contribution of a WD. The reddening they adopted,  $E(B-V)=0.35$ , is more likely the upper limit, and is much larger than the average ( $E(B-V)=0.24$  Bruch & Engel 1994), and the inclination  $i = 18^\circ$  is too low. As a consequence, the mass accretion rate derived by Hamilton et al. is likely overestimated.

We first carry out a modeling of the SWP15078 spectrum assuming  $E(B-V)=0.24$ , and also using a WH disc model, for comparison and consistency with Hamilton et al. We find that a  $1.03M_\odot$  WD accreting at a rate of  $1 \times 10^{-8}M_\odot/\text{yr}$ , with  $i = 41^\circ$  provides a good fit to the spectrum, giving a distance of 402 pc. We display this model in Fig.9.

It is important to note that since the distance to UZ

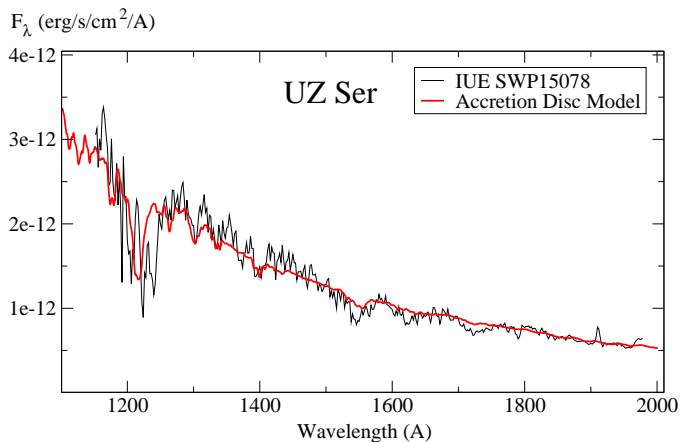


**Figure 9.** The Sep 1981 outburst spectrum of UZ Ser (IUE SWP15078, in black) is modeled with a Wade & Hubeny accretion disc model (in red). The disc model has a  $1.03M_\odot$  WD, a mass accretion rate of  $\dot{M} = 1 \times 10^{-8}M_\odot/\text{yr}$ , and an inclination of  $41^\circ$ , giving a distance of 402 pc. The inner radius of the disc corresponds to a WD radius of 5,000 km, and the outer disc radius is 230,000 km, or about  $0.23a$ .

Ser is only an estimate,  $d \sim 300 - 400$  pc, the uncertainty in the distance translates into an uncertainty in the mass accretion rate  $\dot{M}$  during outburst and an uncertainty in the WD effective surface temperature  $T_{\text{wd}}$  at quiescence. The same is true for the uncertainties in the WD mass ( $M_{\text{wd}} = 0.9 \pm 0.1M_\odot$ ) and the extinction value ( $E(B-V) \approx 0.25 \pm 0.05$ ). The uncertainty in the inclination,  $i = 50^\circ \pm 10^\circ$ , translates only in an uncertainty in  $\dot{M}$ .

We ran additional models within the range of the uncertainties of the parameters. Namely, we ran WH models with  $i = 41^\circ, i = 60^\circ$  for a distance  $d \approx 300, 350, \& 400$  pc. Since the resulting mass accretion rate varies as a function of the WD mass, inclination and distance assumed in the model, we write

$$\dot{M} \equiv \dot{M}(M_{\text{wd}}, i, d).$$

For the above range of parameters it becomes

$$\dot{M}(1M_\odot, 50^\circ \pm 10^\circ, d) \approx (1 \pm 0.25) \left( \frac{d}{350 \text{ pc}} \right)^2 10^{-8} M_\odot \text{yr}^{-1}, \quad (1)$$

where we assume a mean distance of  $\sim 350$  pc,  $1.03M_\odot \approx 1M_\odot$ , and  $41^\circ \approx 40^\circ$ . A change of  $\pm 10^\circ$  (uncertainty) in the inclination produces a change of about  $\pm 1/4$  ( $\pm 0.25$ ) in the mass accretion rate.

Due to the steep slope of the observed SWP IUE spectrum, the best fits are obtained for the models in eq.(1) with a combination of parameters ( $i, d$ ) giving the largest mass accretion rate  $\dot{M} \approx 10^{-8}M_\odot/\text{yr}$  and higher. Namely  $i = 40^\circ$  with  $d = 400$  pc,  $i = 50^\circ$  with  $d \geq 350$  pc, and  $i = 60^\circ$  with  $d \geq 300$  pc, all these models give a goodness of fit similar to the model fit displayed in Fig.9.

The radius of the WH disc model is  $2.3 \times 10^{10}$  cm, corresponding to  $0.23a$  ( $a$  is the binary separation) rather than  $a/3$ . We also tried a disc model we generated from scratch

with the same parameters and with an outer radius  $\sim a/3$ , but the continuum slope of such a model was too shallow. The need for a smaller radius arises from the steep slope of the continuum, which can only be fitted if the colder (outer) region of the disc is cut off.

Since the WD mass of UZ Ser is  $M_{\text{wd}} = 0.9 \pm 0.1 M_{\odot}$ , we also checked a WH disc model with a  $0.8 M_{\odot}$  WD accreting at  $\sim 10^{-8} M_{\odot}/\text{yr}$  and found that it does not provide a continuum slope steep enough to fit the IUE spectrum. As mentioned in section 4.3, all the WH disc models have an outer disc radius cut off at about  $T \sim 10,000$  K (see Fig. 6). To deepen our analysis, we decide to extend the present modeling to the longer wavelength (NUV) by including the LWR segment of the IUE spectrum.

### 5.1.2 The Sep 1981 peak outburst: SWP15078 + LWR11605.

As the WH disc model spectra do not extend beyond  $2000 \text{ \AA}$ , we generated disc models from scratch to check the LW segments of the IUE spectra. We find that the combined IUE SWP15078 + LWR11605 (Sep 22, 1981) spectrum down to  $\sim 3,200 \text{ \AA}$  cannot be fitted with the same disc parameters (i.e.  $M_{\text{wd}} = 1 M_{\odot}$ ,  $\dot{M} = 10^{-8} M_{\odot}/\text{yr}$ ,  $i = 40^\circ$ ,  $R_{\text{disc}} = 0.23a$ ), as the slope of the synthetic spectrum is too shallow in the longer wavelengths compared to the LWR IUE spectrum. To increase the slope of the disc spectrum we have to decrease the outer radius of the disc in the model. We obtain an outer disc radius of  $0.155a$  for a  $1.0 M_{\odot}$  WD accreting at a rate of  $1 \times 10^{-8} M_{\odot}/\text{yr}$ , with  $i = 40^\circ$ , giving a distance of  $\sim 400$  pc. This model fit is displayed in Fig. 10. For a  $0.8 M_{\odot}$  WD disc model, the outer radius of the disc has to be decreased further to  $0.14a$ , giving a distance of 353 pc. Everywhere in the disc the temperature is well above  $10,000$  K, similar to model # 1 in Figs. 6 & 7.

Taking the uncertainties of the parameters into account, we ran models with  $M = 0.8 M_{\odot}$ ,  $1.0 M_{\odot}$ ,  $i = 40^\circ$ ,  $50^\circ$ , and  $60^\circ$ , for a distance  $d \approx 300$ ,  $350$ , and  $400$  pc. Here too the resulting mass accretion rate varies as a function of the parameters ( $d, i$ ), and also as a function of the WD mass  $M_{\text{wd}}$ :

$$\dot{M} \equiv \dot{M}(M_{\text{wd}}, i, d).$$

Explicitly, we have

$$\dot{M}(0.9 \pm 0.1 M_{\odot}, 50^\circ \pm 10^\circ, d) \approx (1.1 \mp 0.1)(1 \pm 0.25) \left( \frac{d}{350 \text{ pc}} \right)^2 10^{-8} M_{\odot} \text{yr}^{-1}. \quad (2)$$

Namely, the change of  $\pm 10^\circ$  (uncertainty) in the inclination produces a change of about  $\pm 1/4$  ( $\pm 0.25$ ) in the mass accretion rate, and a change of  $\pm 0.1 M_{\odot}$  uncertainty in  $M_{\text{wd}}$  produces a change of  $\mp 10^{-9} M_{\odot}/\text{yr}$  in  $\dot{M}$ . Again, due to the steep slope of the observed IUE spectrum, the best fit models are for a combination of parameters ( $i, d$ ) yielding a higher mass accretion rate:  $\dot{M} \approx 10^{-8} M_{\odot}/\text{yr}$  and higher. Considering also a possible uncertainty in the reddening  $E(B - V) \approx 0.25 \pm 0.05$  (see end of section 3.1), we find an additional uncertainty of +60% and -40% in the mass accretion.

The modeling of this first spectrum indicates that the mass accretion rate near peak outburst is of the order of

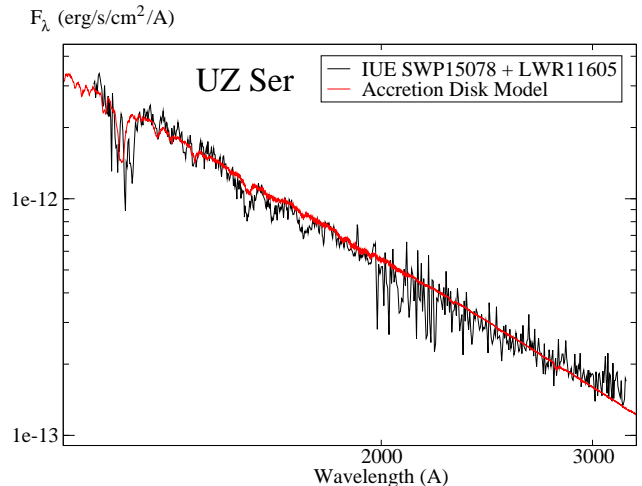


**Figure 10.** The IUE outburst spectrum of UZ Ser (same as in Fig. 9) includes here the longer wavelength (LWR11605) and is fitted with an accretion disc model. The model has  $M_{\text{wd}} = 1.0 M_{\odot}$ ,  $\dot{M} = 10^{-8} M_{\odot}/\text{yr}$ ,  $i = 40^\circ$ , giving a distance  $d \sim 400$  pc. For clarity the axis are logarithmic. Note that in this model the outer radius has been set to  $0.155a$ .

$10^{-8} M_{\odot}/\text{yr}$ , and that the observed spectrum is rather blue. We also obtained that the outer radius of the disc might be rather small, however, in order to decide on the size of the outer disc radius one has to model the hydrogen Balmer region. Unfortunately, no simultaneous optical data exist for the Sep 22, 1981 outburst. An additional factor to take into account in the modeling is the possible contribution of a hot WD which can increase the steepness of the continuum slope to better match the observed (‘blue’) spectrum. The WD is best modeled in quiescence when the contribution from the disc is negligible, and in the present case, the quiescent spectrum itself has a rather steep slope. Consequently, we model the Aug 1982 quiescent spectrum next.

### 5.1.3 The Aug 1982 quiescence.

The optical quiescent spectrum obtained almost simultaneously with the IUE data exhibits many emission lines and a Balmer jump in emission, pointing to an emitting component which we cannot model with a WD stellar photosphere or an optically thick disc. Therefore, we concentrate on modeling the quiescent IUE spectrum (SWP17700 and LWR13960) obtained on Aug 15, 1982. As pointed out earlier, the quiescent IUE spectrum also exhibits a rather steep slope, qualitatively confirming our suspicion that it is dominated by a hot component.

We first ran accretion disc model fits for  $M_{\text{wd}} = 0.8 - 1.0 M_{\odot}$ , and a binary inclination  $i = 40^\circ - 60^\circ$ , and find that disc models yield a mass accretion rate in the range  $1 - 3 \times 10^{-10} M_{\odot}/\text{yr}$ . However, these low mass accretion rate disc spectra do not provide enough flux in the short wavelengths, and are far too ‘red’ compared to the observed spectrum.

Next, we carried out synthetic stellar spectral fits to the quiescent IUE spectrum, fitting mainly the continuum since the Ly $\alpha$  region is contaminated with air-glow. The spectral fits yield a WD temperature  $T_{\text{wd}} \approx 50,000 - 70,000$  K. The

50,000 K WD model provided a fit as good as the 70,000 K WD model, and all the models scaled to the distance we adopted  $d \approx 300 - 400$  pc.

In Fig.11 we display the 60,000 K WD model fit to the IUE quiescent spectrum. The model fit is not very sensitive to the effective surface gravity of the WD, say  $\text{Log}(g) \sim 8.20 - 8.60$ , as the Lyman region is contaminated. At a temperature of 60,000 K, the  $0.9M_{\odot}$  WD has a radius of 6,930 km, giving  $\text{Log}(g) = 8.4$ , and a distance  $d = 360$  pc. For a temperature of 50,000 K the distance decreases to 289 pc, and it increases to 392 pc for  $T=70,000$  K. For a  $1.0M_{\odot}$  WD ( $R_{\text{wd}} = 6,230$  km at 60,000 K) the distance decreases by 10%, and for a  $0.8M_{\odot}$  WD ( $R_{\text{wd}} = 7,709$  km at 60,000 K) the distance increases by 11%.

Overall, the single WD spectral modeling can be summarized as follows: a temperature  $T_{\text{wd}} = 50,000 - 70,000$  K, scaling to a distance  $d = 260 - 435$  pc, for a white dwarf mass  $M_{\text{wd}} = 0.8 - 1.0M_{\odot}$ . The addition of a low mass accretion rate disc with  $\dot{M}_{\text{quies}} \sim 3 \times 10^{-11} - 1 \times 10^{-10} M_{\odot}/\text{yr}$  to the WD model degrades the WD solution. It is, therefore, likely that during quiescence  $\dot{M} < 10^{-10} M_{\odot}/\text{yr}$ , and probably even lower:  $\dot{M} < 3 \times 10^{-11} M_{\odot}/\text{yr}$ . As with most DNe, in quiescence the UV spectrum is likely dominated by emission from the WD, especially if the WD has an elevated temperature.

The elevated temperature implied from the quiescent spectrum, might be a sign that the WD in UZ Ser is still cooling down from a nova explosion. Two other Z Cam systems have detected nova shells: Z Cam (Shara et al. 2007) and AT Cnc (Shara et al. 2012).

The IUE SWP17700 quiescent spectrum was first modeled by Lake & Sion (2001) assuming that the reddening was negligible, it was later remodeled in Urban & Sion (2006) assuming  $E(B-V)=0.30$ . The spectrum was fit with a 99,000 K WD (with a mass  $M_{\text{wd}} = 1M_{\odot}$ ), and a disc (contributing only 1% of the flux) with  $\dot{M} = 10^{-10.5} M_{\odot}/\text{yr}$  and  $i = 18^{\circ}$ , for a distance of 280 pc. The hotter WD temperature they obtained can be attributed to the larger reddening they used. Urban & Sion (2006) did not include the LWR segment in their modeling.

In the optical range, our WD model displays a large discrepancy with the data (see Fig.11) which can be attributed to an additional emitting component, such as a disc wind (Matthews et al. 2015), especially since the hydrogen Balmer lines and Balmer jump are all in emission. Part of the discrepancy, however, could also be due to a problem with the calibration of the optical data as pointed out in Verbunt et al. (1984).

As explained in Sec.4.3, because the spectral coverage in the FUV does not go down the Lyman limit and also because of the relatively low S/N and air-glow contamination of the IUE spectra, we do not consider the possibility of a two-temperature WD model, nor that of a hot boundary layer.

Since the quiescent spectrum was obtained following an outburst for which a spectrum also exists, we decided, for consistency, to model that outburst spectrum taking into account the hot WD component. A decline spectrum was also obtained on Aug 11, 1982, and, therefore, we model both the Aug 1982 outburst and decline spectra next, assuming a WD temperature of 60,000 K and a distance of  $\sim 360$  pc.

#### 5.1.4 The Aug 1982 outburst and decline.

IUE spectra were obtained at outburst on Aug 08, 1982 (SWP17633 & LWR13901), and in decline on Aug 11, 1982 (SWP17661 & LWR13922). Simultaneous optical data were digitally extracted only for the decline phase and no optical spectrum was available for digital extraction for the outburst phase. Based on the results we obtained for the Aug quiescent spectrum, we now include a 60,000 K WD as an addition to the disc modeling for the outburst and decline spectra.

We start by fitting WD+disc models to the decline spectrum. We now use disc models we generated from scratch with an inclination  $i = 50^{\circ}$ , for a WD mass  $M_{\text{wd}} = 0.8M_{\odot}$  &  $M_{\text{wd}} = 1.0M_{\odot}$ .

The outer disc radius is varied to match the Balmer jump and lines of the optical spectrum. We find that the mass accretion rate in decline is  $4.1 \times 10^{-9} M_{\odot}/\text{yr}$  for a  $0.8M_{\odot}$  WD, with an outer disc radius of 0.1a. This model is presented in Fig.11. For a  $1.0M_{\odot}$  WD, the mass accretion rate decreases to  $\sim 2.4 \times 10^{-9} M_{\odot}/\text{yr}$  with an outer disc radius of 0.08a. The very small radius in these models correspond to model # 5 in Fig.6 where the temperature everywhere in the disc is well above 10,000 K. The distance fixed for scaling the two models to the data is  $\sim 350$  pc. Consequently, for a  $0.9 \pm 0.1M_{\odot}$  WD mass, the mass accretion rate in decline is  $\dot{M}_{\text{Decl}} \approx 3.2 \mp 0.9 \times 10^{-9} M_{\odot}/\text{yr}$ , for a distance of 350 pc.

Next, we fit the Aug 1982 outburst spectrum with a combined hot WD + disc model. For a  $0.8M_{\odot}$  WD mass, we find a mass accretion rate of  $\sim 9.2 \times 10^{-9} M_{\odot}/\text{yr}$  (displayed in Fig.11). For a  $1.0M_{\odot}$  WD mass, the mass accretion rate decreases to  $\sim 6.4 \times 10^{-9} M_{\odot}/\text{yr}$ . Here too, the distance was fixed to  $\sim 350$  pc. In other words, for a  $0.9 \pm 0.1M_{\odot}$  WD mass, the mass accretion rate in outburst is  $\dot{M}_{\text{Outb}} \approx 7.8 \mp 1.4 \times 10^{-9} M_{\odot}/\text{yr}$ . Though there is no optical spectrum for the outburst, an outer disc radius of 0.14a provides a better fitting to the near-UV slope for an  $0.8M_{\odot}$  accreting WD, and for an  $1.0M_{\odot}$  accreting WD the outer disc radius is as large as 0.26a similar to model # 1 in Fig.6.

The addition of the 60,000 K WD barely affects the fit of the high mass accretion rate models ( $\sim 10^{-8} M_{\odot}$  in outburst), however, it helps the lower mass accretion rate models ( $\sim 10^{-9} M_{\odot}$  in decline) to better fit the steep slope of the spectral continuum.

To summarize, for a WD mass  $0.9 \pm 0.1M_{\odot}$ , an inclination  $i = 50^{\circ} \pm 10^{\circ}$ , and a distance of  $d$ , we find:

$$\dot{M}_{\text{Outb}} \approx (8 \mp 1.5)(1 \pm 0.25) \left( \frac{d}{350 \text{ pc}} \right)^2 10^{-9} M_{\odot} \text{yr}^{-1},$$

$$\dot{M}_{\text{Decl}} \approx (3 \mp 1)(1 \pm 0.25) \left( \frac{d}{350 \text{ pc}} \right)^2 10^{-9} M_{\odot} / \text{yr}, \quad (3)$$

$\dot{M}_{\text{Quies}} \lesssim 3 \times 10^{-11} M_{\odot}/\text{yr}$ , and  $T_{\text{wd}} \approx 60,000 \pm 10,000$  K, and where we have rounded up the values to 1 or 2 significant figures.

We find a rather small disc radius during decline by fitting the Balmer absorption lines, Balmer jump, and slope of the continuum in the longer wavelength of the IUE spectrum. However, the Balmer  $H_{\alpha}$  and  $H_{\beta}$  lines display broad absorption with narrow emission and we cannot rule out the possibility that the core of the remaining Balmer absorp-

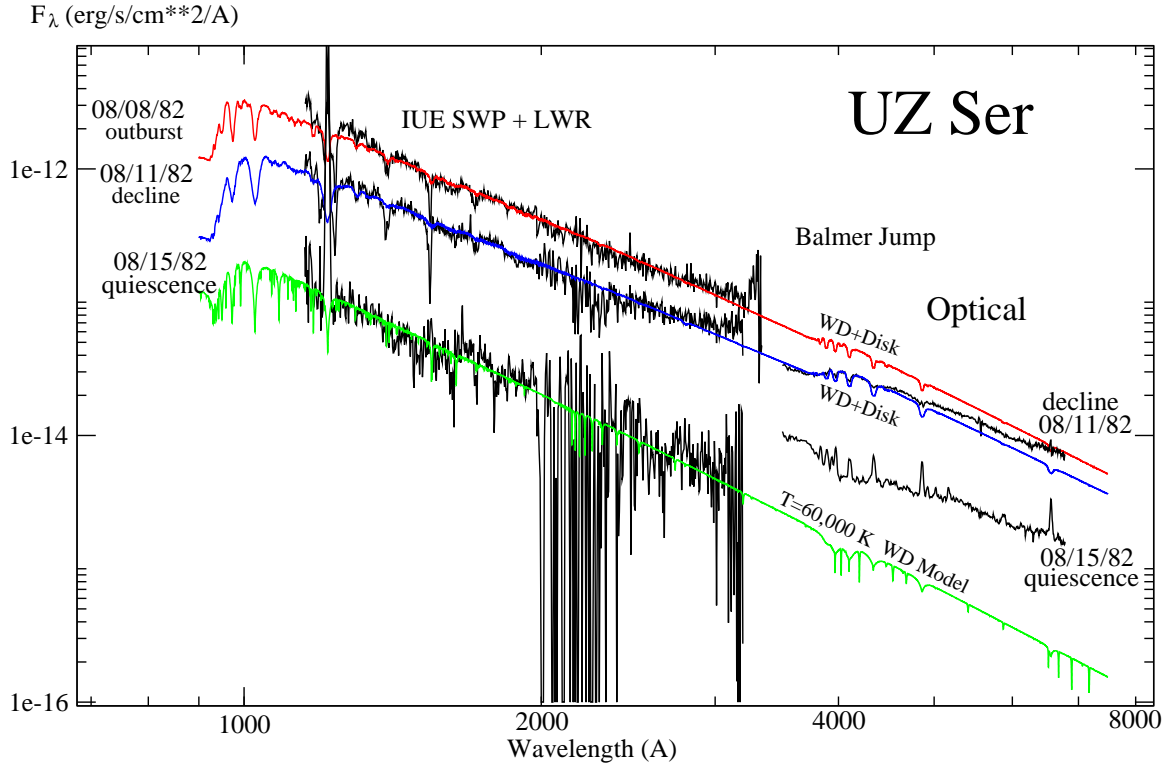


**Figure 11.** The observed Aug 1982 UV-Optical spectra of UZ Ser (solid black lines) are fitted with theoretical model spectra (solid color lines). Simultaneous IUE and optical spectra were obtained in decline (middle) and quiescence (bottom), while the outburst spectrum (top) does not have optical data. In quiescence (Aug 15, 1982) the *IUE* UV spectrum agrees well with a 60,000 K WD (solid green line), but the optical reveals the presence of an emitting component dominated by emission lines. Both the outburst and decline spectra are modeled with the combination a 60,000 K WD and an accretion disc with a mass accretion rate  $\dot{M} \approx 8 \times 10^{-9} M_{\odot}/\text{yr}$  in outburst, and  $\dot{M} \approx 3 \times 10^{-9} M_{\odot}/\text{yr}$  in decline. In order to fit the Balmer jump and the steep slope of the continuum, the outer radius of the disc is set to  $R_{\text{disc}} \approx 0.1a$  in decline, and we assume  $R_{\text{disc}} \approx 0.2a$  in outburst (see text).

tion lines might be partially filled in with emission. CY Lyr presents a better opportunity to model the outer region of the accretion disc.

## 5.2 CY Lyr

### 5.2.1 Peak outburst.

Although the UV and optical outburst spectra of CY Lyr were not obtained simultaneously, they all display a consistent matching flux level (see Fig.4). Consequently, we combine the *IUE* UV spectrum together with the Oct 9, 1982 (Szkody 1985) optical spectrum (z) and Jun 30, 1997 (Thorstensen et al. 1998) optical spectrum (a). We cut off the *IUE* LWR spectrum at 3,000 Å, since the edge of the segment is unreliable, and scaled the optical (a) spectrum to the optical (z) spectrum by multiplying it by 1.05 (see Table 3).

No UV data exist for the quiescent state of CY Lyr, therefore we have no way to model the WD. The optical data at quiescence (Thorstensen et al. 1998) reveals a rather flat continuum dominated by emission lines, and with a flux level of  $\sim 3\%$  that of the outburst flux. The quiescent optical spectrum is believed to be from an M-dwarf and a low- $\dot{M}$  disc component. In the present case we assume that the contribution of the WD to the UV spectrum in outburst is negligible as well, and we model the combined UV + optical spectrum with a disc model only.

The UV region is first fitted with a disc with a given mass accretion rate, then the optical region is fitted by varying the size of the outer radius of the disc. As we decrease the outer radius of the disc, the disc temperature increases, the amplitude of the Balmer Jump in absorption becomes smaller, and the slope of the continuum in the optical becomes steeper.

Since the inclination of the system is unknown, we first assume a median inclination of  $i = 45^\circ$ , and as stated in section 2, we assume a WD with mass of  $0.8M_\odot$ , and a corresponding radius  $R_{\text{wd}} = 7,000$  km (which is also the inner radius of the disc). We find that for these parameters, and with a distance of 489 pc, the UV region matches with a mass accretion rate  $\dot{M} \approx 8.2 \times 10^{-9} M_\odot/\text{yr}$ , while the Balmer jump is matched by truncating the disc at  $R_{\text{disc}} = 0.17a$ . This model is displayed in Fig.12. This disc model is similar to model # 1 in Fig.6, namely the small outer disc radius is needed to match the Balmer jump amplitude. The UV and optical spectra are compatible with a standard disc model and exhibit a spectral slope  $F_\lambda \propto \lambda^{-2.8}$  and  $F_\lambda \propto \lambda^{-3.3}$  respectively.

While we match both the amplitude of the Balmer Jump and the slope of the continuum, the Balmer absorption lines are not matched: the model has deeper lines. However, at peak outburst the observed Balmer absorption lines have emission in their core. In a manner similar to UZ Ser, the emission lines might originate from a disc wind and may also affect the slope and level of the continuum. The optical spectrum obtained during the rise, one day before peak outburst (spectrum b), exhibits deep Balmer absorption lines without peak emission. Therefore, we model this spectrum next.

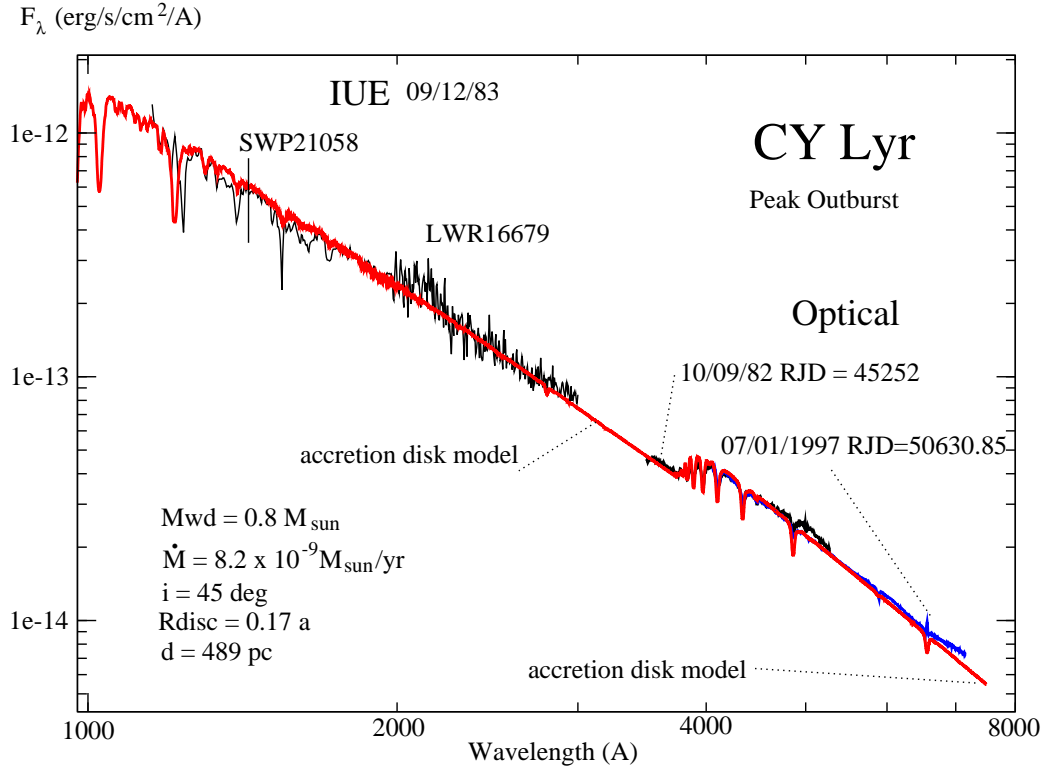


**Figure 12.** The UV and optical spectra of CY Lyr in outburst are fit with an accretion disc model. The 1983 combined IUE SWP + LWR spectrum (1150-3000 Å) is in black, the 1982 optical (z) spectrum ( $\sim 3,500$ -5,300 Å, [Szkody 1985](#)) is in black, and the 1997 optical (a) spectrum ( $\sim 4,000$ -7,200 Å, [Thorstensen et al. 1998](#)) is in blue. The disc model (900-7500 Å) is in red. In order to fit the Balmer jump, the outer disc radius has been set to 0.17a. For an inclination of  $i = 45^\circ$ , one obtains a mass accretion rate of  $\dot{M} = 8.2 \times 10^{-9} M_\odot/\text{yr}$ , and it decreases to  $\dot{M} = 7 \times 10^{-9} M_\odot/\text{yr}$  for an inclination of  $i = 35^\circ$ . There is a small “bump” around 2000 Å which might be mistaken for the 2175 Å ISM dust feature (the polycyclic aromatic hydrocarbons feature (PAH, [Li & Draine 2001](#))) when over-dereddening the spectrum. However, the “bump” is markedly to the left of the PAH feature, an indication that it is due to the low S/N in that region of the IUE LWR segment rather than arising from over-dereddening the spectrum.

### 5.2.2 Rise to outburst.

CY Lyr was caught at the very start of the late June 1997 outburst and optical spectra were obtained almost every hour covering the actual rise from quiescence to outburst (Thorstensen et al. 1998). The optical spectrum (b), obtained one day before the outburst spectrum (a), presents the deepest absorption lines. It has a continuum flux level of  $\sim 66\%$  the level reached at outburst, implying that the mass accretion rate is half than at outburst. With a spectral range from  $\sim 4,000 \text{ \AA}$  to  $\sim 7,200 \text{ \AA}$ , it does not cover the Balmer Jump.

We model this spectrum assuming a WD with a mass  $M_{\text{wd}} = 0.8M_{\odot}$ , a radius  $R_{\text{wd}} = 7,000 \text{ km}$ , and a mass accretion rate  $\dot{M}$  of the order of a few  $10^{-9}M_{\odot}/\text{yr}$ . We have to fit three characteristics of this spectrum: its flux level, its slope, and the depth of its absorption lines. The flux level and the slope are fitted by varying the mass accretion rate and the outer radius of the disc until a fit is found. Then the inclination of the system is varied until the model fits the depth of the observed absorption lines.

We find a mass accretion rate of  $\approx 2.2 \times 10^{-9}M_{\odot}/\text{yr}$  for a distance of  $d = 490 \text{ pc}$ , and the slope of the optical continuum is best fitted when choosing an outer disc radius  $R_{\text{disc}} = 43R_{\text{wd}} = 301,000 \text{ km}$ , or almost exactly  $a/3$ . This disc model corresponds to model # 4 in Fig.6 with an outer disc temperature reaching as low as  $6,000 \text{ K}$ . The inclination,  $i = 35^{\circ} \pm 5^{\circ}$ , was found by matching the  $H_{\gamma}$  absorption lines (the deepest of all the lines) while decreasing the inclination in step of  $5^{\circ}$ . This model fit is displayed in in Fig.13. This spectrum with no emission lines best represents an optically thick standard disc model with deep absorption lines and an outer radius extending all the way to  $\sim a/3$ .

We now remodel the outburst spectrum (Fig.12) with an inclination  $i = 35^{\circ}$ , and find a slightly lower mass accretion rate  $M_{\text{Outb}} \approx 7 \times 10^{-9}M_{\odot}/\text{yr}$ .

For a WD mass of  $0.8 \pm 0.1M_{\odot}$ , and inclination  $i = 35^{\circ} \pm 5^{\circ}$  we have:

$$\dot{M}_{\text{Outb}} \approx (7.0 \pm 1.3)(1.0 \pm 0.1)10^{-9}M_{\odot}\text{yr}^{-1},$$

$$\dot{M}_{\text{rise}} \approx (2.2 \pm 0.5)(1.0 \pm 0.1)10^{-9}M_{\odot}\text{yr}^{-1}. \quad (4)$$

The other optical spectra on the rise to outburst have some emission lines contribution. They also have a low mass accretion rate ( $\sim 10^{-9}M_{\odot}/\text{yr}$  and lower) and, therefore, have a likely contribution from the WD and secondary star for which we do not have enough data to model. In addition, since we do not have any corresponding UV spectra, we do not attempt to model the remaining optical spectra obtained during rise to outburst.

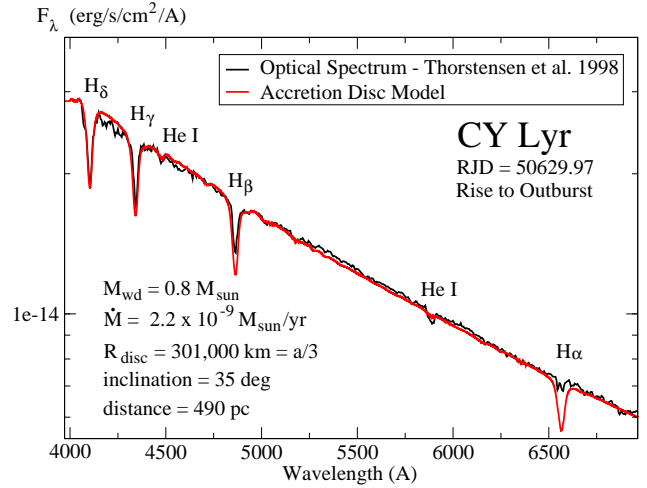


**Figure 13.** The 1997 near-outburst optical (b) spectrum ( $\sim 4,000\text{-}7,200 \text{ \AA}$ , Thorstensen et al. 1998, in black) is fit with an accretion disc model (in red). In order to match the continuum flux level, the mass accretion rate has to be of the order of a few  $10^{-9}M_{\odot}/\text{yr}$ . The outer radius of the disc is dictated by the slope of the continuum and matches the expected theoretical value  $a/3$ . In order to fit the depth of the  $H_{\delta}$  and  $H_{\gamma}$  absorption lines, the inclination has to be set to  $i = 35^{\circ}$ . With these parameters, the resulting mass accretion rate is  $\dot{M} = 2.2 \times 10^{-9}M_{\odot}/\text{yr}$ .

## 6 SUMMARY AND CONCLUSIONS

We carried out a combined UV + optical spectral analysis of two DNe: UZ Ser in outburst, decline, and quiescence, and CY Lyr on the rise to outburst and in outburst. These two CVs are among the very few that actually seem to be in good agreement with the standard disc model (with a UV SED  $F_\lambda \propto \lambda^{-3.0}$  for UZ Ser and  $\propto \lambda^{-2.5}$ , (Godon et al. 2017)).

The archival data of these two systems summarize well the observational properties of DNe. In quiescence, while the UV is mostly dominated by emission from the heated WD, the optical reveals a Balmer jump in emission as well as Balmer emission lines which are not due to the WD. During the rise to outburst, the spectrum becomes bluer: the disc starts to contribute more and more to the UV and optical. The Balmer jump and lines in emission fade and are gradually replaced by a Balmer jump and lines in absorption. The absorption lines are deeper before the outburst peak. During the outburst peak the optical shows emission lines in the bottom of the absorption lines. During decline, the spectrum displays a Balmer jump in absorption, but the jump is not very large. The amplitude of the jump decreased from outburst to decline.

In our modeling, the reduced Balmer jump size (in absorption) is due to a small disc radius ( $R_{\text{disc}} < 0.3a$ ). Using both the IUE and optical data, our results on UZ Ser reveal a 60,000 K WD accreting at a rate of  $\sim 8 \times 10^{-9} M_\odot/\text{yr}$  in outburst,  $\sim 3 \times 10^{-9} M_\odot/\text{yr}$  in decline, and more than 100 times lower in quiescence. The decline phase with simultaneous UV and optical data displays shallow Balmer absorption lines with a small Balmer jump in absorption characteristic of a disc extending only to a radius  $\sim 0.1a$ . The outburst phase may have a larger radius of the order of  $\sim 0.2a$ . CY Lyr reveals a similar picture with a mass accretion rate of  $\sim 8 \times 10^{-9} M_\odot/\text{yr}$  in outburst, and  $\sim 2 \times 10^{-9} M_\odot/\text{yr}$  on the rise to outburst, but the lack of UV data in quiescence prevents us from assessing the WD temperature. The modest Balmer jump in absorption during outburst gives an outer disc radius of  $\sim 0.17a$ . However, the optical data during rise to outburst (one day before the outburst peak) displaying the deepest absorption lines, gives a disc radius of  $0.3a$ .

Overall, the results of our spectral analysis show that during a dwarf nova cycle the UV-optical spectrum agrees well with the standard disc model *just before the peak of the outburst*. If the depth of the Balmer jump and lines in absorption in UZ Ser is solely due to the outer disc radius at a fixed inclination, as in our modeling, then, during outburst and decline the disc has a radius smaller than expected ( $\sim 0.17a$ ), and one day before the peak outburst, towards the end of the rise, the disc has a radius of  $\sim 0.3a$ . This consists in a  $\sim 43\%$  change in the disc size relative to its maximum size. This is in *qualitative* agreement with the disc instability model (DIM) for dwarf nova outbursts (Hameury et al. 1998), but quantitatively it over-estimates the relative change. Simulations of the DIM when taking into account mass-transfer fluctuation due to irradiation of the secondary (Hameury et al. 2000), or additional dissipation heating (Buat-Ménard et al. 2001, stream impact, tidal-torque - see Lasota (2001) for a review), exhibit a change in radius size of up to only  $\sim 25\%$ .

We note that during outburst, the disc models had a temperature ( $T \sim 7000$  K and up) everywhere consistent

with the upper branch of the S-curve of the DIM; during the late rise the disc model had a minimum temperature reaching 6,000 K; and there was no need for models with an outer disc temperature below that ( $T \sim 3500 - 6000$  K, such as model # 3 in Fig.6) as found in the lower branch of the S-curve of the DIM (Hassall et al. 1985).

The observed reduced Balmer jump size and depth of the Balmer absorption lines could also be due, in part, to a disc wind causing core emission (as in nova-likes Matthews et al. 2015). In quiescence, Balmer emission lines are dominating the spectrum, as the system rises to outburst, the slope of the increasing spectrum steepens and core emission is seen at the bottom of the absorption lines. During late rise the absorption lines are deeper and core emission seems minimal or null. As the system reaches its outburst peak the depth of the absorption lines is again reduced by core emission. We do not rule out the existence of such a wind which also reduces the slope of the UV and optical continua. Both the wind and radius of the disc have to be taken into account for a more realistic modeling of disc-dominated CV systems - including nova-likes.

Only at the very end of the rise to outburst does a DN system have a spectrum consistent with an actual steady-state standard accretion disc. We emphasize that optical data obtained at the end of the rise to outburst, especially when combined with available UV data, are extremely valuable for modelling dwarf novae, as they allow a determination of the inclination of the system, the mass accretion rate and the outer disc radius.

## ACKNOWLEDGEMENTS

We wish to thank an anonymous referee for her/his pertinent report and constructive criticism, which helped improve the manuscript. This work is supported by the National Aeronautics and Space Administration (NASA) under grant number NNX17AF36G issued through the Office of Astrophysics Data Analysis Program (ADAP) to Villanova University. PS acknowledges support from NSF AST-1514737. We have made use of online data from the AAVSO, and we are thankful to the AAVSO staff and members worldwide.

## REFERENCES

- Baker, R.H., & Kiefer, L. 1942, ApJ, 96, 224
- Brown, A.G.A., Vallenari, A., Prusti, T., de Bruijne, J.H.J., Babusiaux, C., et al. 2018, A&A, 616, 1
- Bruch, A., & Engel, A. 1994, A&AS, 104, 79
- Buat-Ménard, V., Hameury, J.-M., Lasota, J.-P. 2001, A&A, 366, 612
- Cardelli, J.A., Clayton, G.C. Mathis, J.S. 1989a, ApJ, 345, 245
- Cardelli, J.A., Clayton, G.C. Mathis, J.S. 1989b, Interstellar Dust, 134, 5
- Darnley, M.J., Hounsell, R., Godon, P., Perley, D.A., Henze, M. et al. 2017, ApJ, 847, 35
- la Dous, C. 1989a, MNRAS, 238, 935
- la Dous, C. 1989b, A&A, 1989, 211, 131
- la Dous, C. 1991, A&A, 252, 100
- Dyck, G.P. 1987, J.Am.Assoc.Var.Star Obs., 16, 91
- Dyck, G.P. 1989, J.Am.Assoc.Var.Star Obs., 18, 105
- Echevarría, J., and Costero, R. 1983, *Revista Mexicana de Astronomía y Astrofísica*, 8, 141

- Echevarría, J. 1988, *Revista Mexicana de Astronomía y Astrofísica*, 16, 37
- Echevarría, J., Jones, D.H.P., Wallis, R.E., Mayo, S.K., Hassall, B.J.M., et al. 1981, *MNRAS*, 197, 565
- Echevarría, J., & Michel, R. 2007, *Revista Mexicana de Astronomía y Astrofísica*, 43, 291
- Eyer, L., Rimoldini, L., Audard, M., Anderson, R.I., Nienartowicz, K., et al. 2018, arXiv180409382, *Gaia Data Release 2: Variable STars in the colour-magnitude diagram*, A&A, in press (special issue for the Gaia DR2)
- Fitzpatrick, E.L., & Massa, D. 2007, *ApJ*, 663, 320
- Godon, P. 2019, *ApJ*, 870, 112
- Godon, P., Sion, E.M., Balman, S., Blair, W.P. 2017, *ApJ*, 846, 52
- Godon, P., Sion, E.M., Levay, K., Linnell, A.P., Szkody, P., Barrett, P.E., Hubeny I., & Blair, W.P. 2012, *ApJS*, 203, 29
- Godon, P., Sion, E.M., Williams, R.E., & Starfield, S. 2018, *ApJ*, 862, 89
- Goodman, J. 1993, *ApJ*, 406, 596
- Greenberg, J.M., & Chlewicki, G. 1983, *ApJ*, 272, 563
- Hameury, J.-M., Lasota, J.-P., Warner, B. 2000, A&A, 353, 244
- Hameury, J.-M., Menou, K., Dubus, G., Lasota, J.-P., Huré, J.-M., 1998, *MNRAS*, 298, 1048
- Hamilton, R., et al. 2007, *ApJ*, 667, 1139
- Haug, K. 1987, *ApJS*, 130, 91
- Herbig, G.H. 1944, *PASP*, 56, 230
- Honeycutt, R.K., Robertson, J.W., Turner, G.W., & Mattei, J.A. 1998, *PASP*, 110 676
- Horne, K., Marsh, T.R., Cheng, F.H., Hubeny, I., Lanz, T. 1994, *ApJ*, 426, 294
- Hubeny, I. 1988, *Comput.Phys.Commun.*, 52, 103
- Hubeny, I., & Lanz, T. 1995, *ApJ*, 439, 875
- Hubeny, I., & Lanz, T. 2017a, *A brief introductory guide to TLUSTY and SYNPEC* arXiv:1706.01859
- Hubeny, I., & Lanz, T. 2017b, *TLUSTY User's Guide II: Reference Manual* arXiv:1706.01935
- Hubeny, I., & Lanz, T. 2017c, *TLUSTY User's Guide III: Operational Manual* arXiv:1706.01937
- Hubeny, I., Lanz, T., & Jeffrey, S. 1994, *St. Andrews Univ. Newsletter on Analysis of Astronomical Spectra*, 20, 30
- Idan, I., Lasota, J.-P., Hameury, J.-M., Shaviv, G. 2010, A&A, 519, 117
- Hassall, B.J.M., Pringle, J.E., Schwarzenberg-Czerny, A., Wade, R.A., Whelan, J.A.J., & Hill, P. 1983, *MNRAS*, 203, 865
- Hassall, B.J.M., Pringle, J.E., & Verbunt, F. 1985, *MNRAS*, 216, 353
- Knigge, C., Long, K.S., Blair, W.P., Wade, R.A. 1997, *ApJ*, 476, 291
- Knigge, C., Long, K.S., Wade, R.A., Baptista, R., Horne, K., Hubeny, I., Rutten, R.G.M. 1998, *ApJ*, 499, 414
- Kurucz, R.L. 1979, *ApJS*, 40, 1
- Lake, J., & Sion, E.M. 2001, *AJ*, 122, 1632
- Lasota, J.-P. 2001, *New Astronomy Review*, 45, 449
- Li, A., & Draine, B.T. 2001, *ApJ*, 554, 778
- Linnell, A.P., Godon, P., Hubeny, I., Sion, E.M., & Szkody, P. 2007, *ApJ*, 662, 1204
- Linnell, A.P., Godon, P., Hubeny, I., Sion, E.M., Szkody, P., Barrett, P.E. 2008, *ApJ*, 676, 1226
- Linnell, A.P., Godon, P., Hubeny, I., Sion, E.M., Szkody, P., Barrett, P.E. 2009, *ApJ*, 703, 1839
- Linnell, A.P., Godon, P., Hubeny, I., Sion, E.M., & Szkody, P. 2010, *ApJ*, 719, 271
- Linnell, A.P., DeStefano, P., Hubeny, I. 2012, *PASP*, 124, 885
- Long, K.S., Blair, W.P., Davidsen, A.F., Bowers, C.W., Van Dyke Dison, W., et al. 1991, *ApJ*, 381, L25
- Long, K.S., Gänsicke, B.T., Knigge, C., Froning, C.S., Monard, B. 2009, *ApJ*, 697, 1512
- Long, K.S., Wade, R.A., Blair, W.P., Davidsen, A.F., & Hubeny, I. 1994, *ApJ*, 426, 704
- Luri, X., Brown, A.G.A., Sarro, L.M., Arenou, F., Bailer-Jones, C.A.L., et al. 2018, A&A, 616, 9 *Gaia Data Release 2, Using Gaia Parallaxes*
- Lynden-Bell, D. 1969, *Nature*, 223, 690
- Lynden-Bell, D., & Pringle, J.E. 1974, *MNRAS*, 168, 303
- Mathis, J.S. 1990, *ARA&A*, 28, 37
- Matthews, J.H., Knigge, C., Long, K.S., Sim, S.A., Higginbottom, N. 2017, *MNRAS*, 450, 3331
- Morales-Durán, C., Rodrigo-Blanco, C., Cabo-Cubeiro, P., Llorente-de Andrés, F., & Solano-Márquez, E. 2015, *Memorie della Società Astronomica Italiana*, Vol.86, p.639
- Mummery, A., & Balbus, S.A. 2019, *MNRAS*, 489, 132
- Nixon, C.J., & Pringle, J.E. 2019, A&A, 628, 121
- Paczyński, B. 1977, *ApJ*, 216, 822
- Pala, A.F., Gänsicke, B.T., Townsley, D. & 28 authors, 2017, *MNRAS*, 466, 2855
- Panek, R.J. 1979 *ApJ*, 234, 1016
- Pringle, J.E. 1981, *ARA&A*, 19, 137
- Prusti, T., de Bruijne, J.H.J., Brown, A.G.A., Vallenari, A., Babusiaux, C., et al. 2016, A&A, 595, 1
- Puebla, R.E., Diaz, M.P., Hubeny, I. 2007, *ApJ*, 134, 1923
- Sassee, T.P., Hurwitz, M., Dixon, W.V., Airieau, S. 2002, *ApJ*, 566, 267
- Savage, B.D. Mathis J.S. 1979, *ARAA*, 17, 73
- Schlafly, E.F., & Finkbeiner, D.P. 2011, *ApJ*, 737, 103
- Schlegel, D.J., Finkbeiner, D.P., & David, M. 1998, *ApJ*, 500, 525
- Seaton, M.J. 1979, *MNRAS*, 187, 73
- Sevelli, P., & Gilmozzi, R. 2013, A&A, 560, 49
- Shakura, N.I., & Sunyaev, R.A. 1973, A&A, 24, 337
- Shapovalov, D.S., & Vishniac, E.T. 2011, *ApJ*, 738, 66
- Shara, M.M., Martin, C.D., Seibert, M., Rich, R.M., Salim, S. et al. 2007, *Nature*, 446, 159
- Shara, M.M., Mizusawa, T., Wehinger, P., Zurek, D., Martin, C. et al. 2012, *ApJ*, 758, 121
- Shaviv, G., & Wehrse, R. 1991, A&A, 251, 117
- Smith, L.J., Crowther, P.A., & Prinja, R.K. 1994, A&A, 281, 833
- Szkody, P. 1985, *AJ*, 90, 1837
- Szkody, P., & Mattei, J.A. 1984, *PASP*, 96, 988
- Thorstensen, J.R., Taylor, C.J., & Kemp, J. 1998, *PASP*, 110, 1405
- Urban, J., & Sion, E.M. 2006, *ApJ*, 642, 1029
- Verbunt, F. 1987, A&AS, 71, 339
- Verbunt, F., Pringle, J.E., Wade, R.A., Echevarría, J., Jones, D.H.P., et al. 1984, *MNRAS*, 210, 197
- Wade, R.A. 1984, *MNRAS*, 208, 381
- Wade, R.A. 1988, *ApJ*, 335, 394
- Wade, R.A., & Hubeny, I. 1998, *ApJ*, 509, 350
- Warner, B. 1995, *Cataclysmic Variable Stars*, CUP
- Williams, G. 1983, *ApJS*, 52, 523
- Zorotovic, M., Schreiber, M.R., Gänsicke, B.T. 2011, A&A, 536, 42

This paper has been typeset from a  $\text{\TeX}/\text{\LaTeX}$  file prepared by the author.